

Cite this: *Chem. Sci.*, 2021, 12, 3768

All publication charges for this article have been paid for by the Royal Society of Chemistry

# Amyloid binding and beyond: a new approach for Alzheimer's disease drug discovery targeting A $\beta$ –PrP<sup>C</sup> binding and downstream pathways†

James D. Grayson,<sup>a</sup> Matthew P. Baumgartner,<sup>b</sup> Cleide Dos Santos Souza,<sup>a</sup> Samuel J. Dawes,<sup>ac</sup> Imane Ghafir El Idrissi,<sup>d</sup> Jennifer C. Louth,<sup>a</sup> Sasha Stimpson,<sup>a</sup> Emma Mead,<sup>e</sup> Charlotte Dunbar,<sup>e</sup> Joanna Wolak,<sup>e</sup> Gary Sharman,<sup>e</sup> David Evans,<sup>id e</sup> Anastasia Zhuravleva,<sup>c</sup> Margarita Segovia Roldan,<sup>g</sup> Nicola Antonio Colabufo,<sup>id df</sup> Ke Ning,<sup>g</sup> Claire Garwood,<sup>g</sup> James A. Thomas,<sup>id a</sup> Benjamin M. Partridge,<sup>id a</sup> Antonio de la Vega de Leon,<sup>id h</sup> Valerie J. Gillet,<sup>h</sup> Amélia P. Rauter,<sup>id i</sup> and Beining Chen,<sup>id \*a</sup>

Amyloid  $\beta$  oligomers (A $\beta$ ) are the main toxic species in Alzheimer's disease, which have been targeted for single drug treatment with very little success. In this work we report a new approach for identifying functional A $\beta$  binding compounds. A tailored library of 971 fluorine containing compounds was selected by a computational method, developed to generate molecular diversity. These compounds were screened for A $\beta$  binding by a combined <sup>19</sup>F and STD NMR technique. Six hits were evaluated in three parallel biochemical and functional assays. Two compounds disrupted A $\beta$  binding to its receptor PrP<sup>C</sup> in HEK293 cells. They reduced the pFyn levels triggered by A $\beta$  treatment in neuroprogenitor cells derived from human induced pluripotent stem cells (hiPSC). Inhibitory effects on pTau production in cortical neurons derived from hiPSC were also observed. These drug-like compounds connect three of the pillars in Alzheimer's disease pathology, *i.e.* prion, A $\beta$  and Tau, affecting three different pathways through specific binding to A $\beta$  and are, indeed, promising candidates for further development.

Received 3rd September 2020

Accepted 8th January 2021

DOI: 10.1039/d0sc04769d

rsc.li/chemical-science

## Introduction

Dementia is a family of age-related, incurable, and debilitating conditions which are characterised by a serious loss of cognitive ability beyond normal ageing that affects both men and women.<sup>1</sup> Currently, 50 million people are suffering from dementia globally and this number is expected to increase to

over 152 million by 2050.<sup>2</sup> The global healthcare cost of dementia in 2018 escalated to \$1 trillion dollars and is expected to double to \$2 trillion by 2030. This hampers social and economic development and overwhelms health and social services, including the long-term care service.<sup>2</sup>

Alzheimer's disease (AD) accounts for about 80% of all dementia cases. The onset of AD normally occurs in the later stages of human life (60–70 years old) and is triggered by many different pathological and environmental factors. The accumulations of the protein fragment  $\beta$ -amyloid (called  $\beta$ -amyloid plaques) deposited outside neurons, and an abnormal form of the protein tau (called tau tangles) accumulated inside neurons are two of several pathological changes associated with AD.<sup>3</sup>  $\beta$ -amyloid plaques are believed to contribute to cell death by interfering with neuron-to-neuron communication at synapses,<sup>4–9</sup> while tau tangles block the transport of nutrients and other essential molecules inside neurons.<sup>10,11</sup> Most AD cases are of sporadic origin and the onset of cognitive behavioural impairment occurs well before clinical symptoms are seen.<sup>12</sup>

Over the past three decades, no single curative treatment for AD has been developed although some reached advanced clinical trial stages. For example, solanezumab, a monoclonal antibody targeting the central epitope of monomeric amyloid- $\beta$ ,

<sup>a</sup>Department of Chemistry, University of Sheffield, Brookhill, Sheffield S3 7HF, UK. E-mail: b.chen@sheffield.ac.uk

<sup>b</sup>Computational Chemistry and Cheminformatics, Eli Lilly and Company, Lilly Biotechnology Center, San Diego, CA 92121, USA

<sup>c</sup>Faculty of Biological Sciences, University of Leeds, Leeds LS2 9JT, UK

<sup>d</sup>Univ Bari, Biofordrug, Via Edoardo Orabona 4, I-70125 Bari, Italy

<sup>e</sup>Computational Chemistry and Cheminformatics, Eli Lilly and Company, Erl Wood, Windlesham, GU20 6PH, UK

<sup>f</sup>Univ Bari, Dipartimento Farm Sci Farmaco, Via Edoardo Orabona 4, I-70125 Bari, Italy

<sup>g</sup>Sheffield Institute of Translational Neuroscience, University of Sheffield, Sheffield S10 2HQ, UK

<sup>h</sup>Information School, University of Sheffield, Sheffield S1 4DP, UK

<sup>i</sup>Centro de Química Estrutural, Faculdade de Ciências, Universidade de Lisboa, ED C8, 5 piso, 1749-016 Lisboa, Portugal

† Electronic supplementary information (ESI) available. See DOI: 10.1039/d0sc04769d



KLFFFAED, with picomolar affinity, was developed by Eli Lilly in 2002.<sup>13–15</sup> Solanezumab entered Phase II clinical trials in 2006, and was withdrawn from development in 2018 after over 15 years of studies and a billion dollar investment.<sup>16</sup> The latest casualty is aducanumab from Biogen which is another monoclonal antibody targeting the aggregated forms of A $\beta$  amyloid. Biogen halted development of the drug in March 2019 after preliminary data from two Phase III trials suggested it would not meet the primary endpoint. However, in October 2019 the company announced their intention to seek regulatory approval, following a reanalysis of the data.<sup>17</sup>

There are many reasons for such a high failure rate in AD drug discovery and development.<sup>18</sup> The most pressing one is that the vast majority of current therapeutic approaches as demonstrated above only focus on a single target (mainly around amyloid beta) which alone is insufficient to cure AD, a complex disease with multiple causes.<sup>19</sup> While amyloid beta is still a viable and clinically validated anti-oligomeropathy drug target, we believe that looking beyond just amyloid binding, *i.e.* the downstream effects of A $\beta$  rather than on its accumulation and aggregation alone, especially how the binding affects its binding partners and other related signalling pathways, may be advantageous in improving the success rate of drug discovery for AD and produce urgently needed therapies.

It is commonly accepted that pathogenic amyloid beta (A $\beta$  or A $\beta$ eta), A $\beta$ <sub>1–42</sub>, is the main component of the amyloid plaques found in the brains of Alzheimer patients.<sup>4,16</sup> This peptide is the product of proteolytic cleavage of the amyloid precursor protein (APP) by  $\beta$ -secretase and  $\gamma$ -secretase.<sup>20,21</sup> Monomeric A $\beta$ <sub>1–42</sub> can aggregate to form flexible soluble oligomers which may exist in several forms from small oligomers to fibrils.<sup>8</sup> The formation of oligomeric species precedes the formation of amyloid plaques and the presence of protofibrils and oligomers correlates well with the neurotoxicity showing that oligomers have played a critical role in the pathogenesis and progression of AD (oligomeropathy).<sup>22–24</sup> In addition, the misfolded oligomers (known as “seeds”) can induce A $\beta$  molecules to also take the misfolded oligomeric form, leading to a chain reaction akin to a ‘prion’ infection.<sup>25–27</sup> The other key protein, tau, which is also involved in AD forms ‘prion-like’ misfolded oligomers (Tauopathy).<sup>28</sup> It is also believed that there is a connection between oligomeropathy and tauopathy, *i.e.* misfolded A $\beta$  oligomers can induce tau to misfold.<sup>10,23</sup>

In addition, several receptors for A $\beta$ <sub>1–42</sub> oligomers (A $\beta$ o will be used throughout this paper unless otherwise stated) at synapses were discovered. Notably, the cellular prion protein (PrP<sup>C</sup>) has high affinity for A $\beta$ o.<sup>29</sup> PrP<sup>C</sup>, a glycosylphosphatidylinositol (GPI)-anchored protein of 231 amino acids encoded by the *PrnP* gene located on chromosome 20 in humans, is widely expressed in the central nervous system during early development, and in adult neurons and glial cells. In the adult brain, maximal *PrnP* mRNA expression is observed in the neocortex and cerebellum. Although its involvement in transmissible spongiform encephalopathies is well known, PrP<sup>C</sup> is thought to be related to several normal and abnormal physiological processes.<sup>11</sup> In AD, conditional deletion of the

*PrnP* gene by anticancer drug, tamoxifen,<sup>30,31</sup> rescued synapse loss in APP/PS1 mice models. The interaction between PrP<sup>C</sup> and A $\beta$ o appears to be involved in maintaining cognitive impairment in later stages of AD and endogenous or, synthetic ligands of PrP<sup>C</sup> interrupt A $\beta$ o mediated signalling and prevent neurotoxicity in neurons.<sup>12,29,32</sup> Evidence also shows that PrP<sup>C</sup> deletion influences tau hyperphosphorylation because Fyn has been linked to somatodendritic accumulation of Tau. Therefore, cellular prion protein, PrP<sup>C</sup>, plays a vital role in the central dogma of AD aetiology connecting oligomeropathy with Tauopathy. Therefore, A $\beta$  oligomers, PrP<sup>C</sup>, Fyn and Tau could all become potential polypharmacological drug discovery targets for AD.<sup>33</sup>

Here, we present a combined computational, biophysical, biochemical, and cellular effort in developing novel drug discovery approaches against AD. We developed a virtual screening strategy for identifying putative A $\beta$ o binders. We identified compounds reported as inhibitors for A $\beta$  in the public domain and in the literature and used these compounds to search a library of fluorine-containing compounds using a fragment-based approach. Sub-libraries of compounds suggested from virtual screening were examined in a <sup>19</sup>F NMR assay to identify compounds that bind to A $\beta$ o. The hit compounds were further tested in a number orthogonal NMR based assays to confirm their specific binding to A $\beta$ o.

Furthermore, we have identified several promising chemical scaffolds and tested them in cellular assays to validate their bindings and biological activities. We have developed a cellular-based A $\beta$ o–PrP<sup>C</sup> binding assay using HEK293 cell line. The selected compounds were also tested in more disease relevant models using induced human pluripotent stem cells (ihPSC) for their abilities in inhibiting hyperphosphorylations of Fyn and Tau. Together with an enzymatic BACE assay, these compounds were shown to specifically bind to A $\beta$ o, disrupt the A $\beta$ o–PrP<sup>C</sup> interaction, inhibit hyperphosphorylation of Fyn and Tau.

## Results and discussion

### Computational library design

**Designing fluorine-containing fragment library.** The design of a compound library targeting A $\beta$ o was inspired by the work reported by Joshi *et al.*<sup>34</sup> who used a computational fragment-based approach to produce small molecule libraries targeting intrinsically disordered proteins from known anti-amyloid compounds. In order to generate a more specific and focused library for subsequent binding studies against A $\beta$ o using <sup>19</sup>F NMR, a computational pipeline was developed as illustrated (Fig. 1a) and described in detail in the Methods section.

We identified 151 known A $\beta$ o inhibitors from the literature and public databases (ESI Table 1†). These seed compounds were fragmented and then these fragments (after filtering very simple fragments like phenyl rings) were used to perform a substructure search on a tailored chemical library consisting of 7220 fluorine-containing compounds. This library was a subset of a larger library of 73 848 compounds constructed from public databases such as ChEMBL, PubChem, Drugbank,



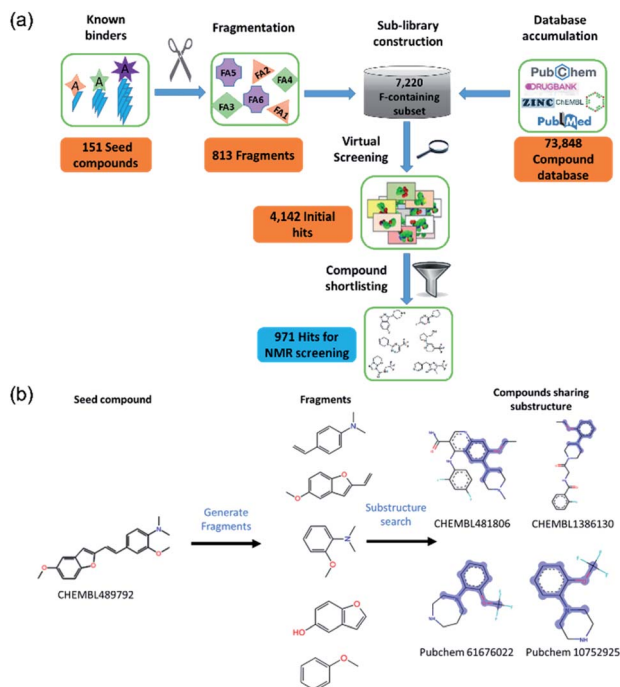


Fig. 1 Computational design of fluorine containing anti-oligomeropathy compound library. (a) Flowchart for database construction and screening cascade. (b) A schematic illustration of computational fragment-based approach from a known A $\beta$  binder CHEMBL489792.

and ZINC. The sub-library consists of compounds containing at least one fluorine atom and the compounds were available in Lilly's internal inventory (to allow for rapid procurement of

the compounds). This fluorine subset was specifically selected to allow  $^{19}\text{F}$  NMR screening to be employed.<sup>35</sup>

The initial substructure search against the F-containing chemical library yielded 4142 initial hits from which 2000 diverse compounds were selected. Further assessment on their predicted solubility resulted in 971 compounds which were taken forward into the  $^{19}\text{F}$  NMR screening (ESI Table 2 $\dagger$ ). The design cascade can be illustrated using a known A $\beta$  binder CHEMBL489792 as an example (Fig. 1b). CHEMBL489792 is an aminostyrylbenzofuran derivative which was reported to be a potent inhibitor for A $\beta$  fibril formation with  $\text{IC}_{50}$  of 0.07 mM in thioflavin T (ThT) assay.<sup>36</sup> Fragments were generated from this compound and these fragments were screened against the compiled fluorine-containing database subset resulting in compounds that share the identified fragment substructures.

**Hit expansion by similarity search.** A similarity search against the main database of 73 848 compounds was applied to the 8 hits from the initial  $^{19}\text{F}$  NMR screening in order to produce more analogues in the hit expansion exercise. 36 fluorine and non-fluorine containing structural analogues were selected computationally (ESI Table 4 $\dagger$ ). These compounds were screened in a competition assay using the  $^{19}\text{F}$  NMR technique employed in the primary screening. This round of hit expansion exercise yielded 6 more hit compounds (Table 2). All 14 hits were then further validated and characterised by STD NMR to give 9 confirmed hits of which 6 were progressed to biological validation.

## NMR screening and characterisation of binding

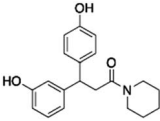
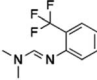
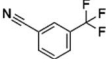
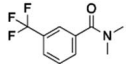
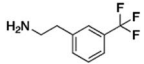
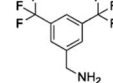
**A $\beta$  oligomer preparation and characterisation.** The A $\beta_{1-42}$  oligomers (abbreviated as A $\beta$ o unless otherwise stated) used in

Table 1  $^{19}\text{F}$  NMR screening data for 27 hit compounds

Entry	Sub-library location	Public ID	$^{19}\text{F}$ NMR sublibrary Screening					$^{19}\text{F}$ NMR individual experiment					$^{19}\text{F}$ NMR scrambled peptide experiment				
			Chemical Shift	Height Reduction	Noise	Reduction /Noise	Height Decrease (%)	Chemical Shift	Height Reduction	Noise	Reduction /Noise	Height Decrease (%)	Chemical Shift	Height Reduction	Noise	Reduction /Noise	Height Decrease (%)
1	1004	CHEMBL1302101	-63.4125	402.06	37.49	10.72	8.33	-64.6565	438.7483	49.62	8.84	9.17	-64.6565	241.41	49.62	4.87	5.09
2	1007	PBCHM13530069	-75.2216	469.36	37.06	12.67	21.48	-117.0970	1046.4400	46.14	22.68	40.04	-117.0970	758.48	46.14	16.44	29.02
3	1009	CHEMBL1673279	-119.6377	415.65	38.79	10.72	18.88	-116.9740	731.4906	49.01	14.93	32.07	-116.9740	-358.1	49.01	-7.31	-30.11
4	1028	PBCHM4151894	-60.6151	998.68	36.74	27.18	34.78	-75.4117	402.0800	55.39	7.26	26.76	-75.4117	704.93	55.39	12.73	46.91
5	1031	PBCHM4284201	-62.3034	353.18	36.98	9.55	8.82	-61.5743	177.1300	47.70	3.71	3.33	-61.5743	149.3	47.70	3.13	2.82
6	1032	ZINC19735908	-62.6422	248.07	37.97	6.53	7.04	-60.9935	-5.8595	43.59	-0.13	-0.12	-60.9935	290.04	43.59	6.65	5.98
7	1034	CHEMBL1499171	-116.8663	467.98	37.19	12.58	7.82	-75.2216	76.7367	36.61	2.10	20.50	-75.2216	-985.78	36.61	-26.93	-16.89
8	1035	CHEMBL24458	-62.2623	369.44	44.03	8.39	12.64	-61.9927	2134.5300	41.21	51.80	56.73	-61.9927	287.69	41.21	6.98	7.65
9	1042	ZINC02243315	-117.0970	152.10	57.81	2.63	13.52	-114.1509	-3.6773	51.32	-0.07	-0.22	-114.1509	64.94	51.32	1.27	3.69
10	1043	ZINC04653292	-109.0352	228.62	37.26	6.14	5.90	-74.1409	231.6288	48.91	4.74	4.29	-74.1409	216.45	48.91	4.43	3.94
11	1043	PBCHM4680099	-61.5743	153.59	37.04	4.15	15.93	-115.3825	152.7545	74.29	2.06	9.71	-115.3825	142.93	74.29	1.92	8.78
12	1045	ZINC02382246	-114.1509	154.73	37.00	4.18	4.85	-57.6477	-9.2234	48.12	-0.19	-0.17	-57.6477	47.59	48.12	0.99	0.89
13	1045	PBCHM57487213	-64.6565	392.67	34.75	11.30	17.39	-62.2768	865.2674	51.91	16.67	21.93	-62.2768	-85.75	51.91	-1.65	-2.26
14	1046	CHEMBL1351172	-61.9927	171.47	36.06	4.76	9.44	-79.7360	271.1473	55.78	4.86	9.38	-79.7360	-48.07	55.78	-0.86	-1.62
15	1048	PBCHM3049683	-60.9935	342.06	36.04	9.49	11.62	-62.6422	539.3773	42.10	12.81	9.32	-62.6422	-223.04	42.10	-5.30	-3.54
16	1053	PBCHM83397192	-62.7087	198.86	36.04	5.52	5.35	-60.6151	114.6180	41.20	2.78	2.54	-60.6151	215.82	41.2	5.24	4.55
17	1055	PBCHM120765	-79.7360	308.27	36.01	8.56	7.30	-62.2623	130.2060	48.67	2.68	2.59	-62.2623	-128.09	48.67	-2.63	-2.45
18	1055	PBCHM2738092	-57.6477	313.95	35.81	8.77	46.15	-109.0352	271.1100	49.68	5.46	79.80	-109.0352	236.01	49.68	4.75	69.47
19	1057	PBCHM609266	-74.1409	306.18	34.34	8.92	16.76	-73.1952	1707.0500	61.73	27.65	58.50	-73.1952	321.77	61.73	5.21	11.03
20	1058	PBCHM13486675	-116.9740	300.36	36.48	8.23	9.81	-63.4125	1876.7700	40.50	46.34	46.38	-63.4125	303.3	40.5	7.49	7.5
21	1059	PBCHM33678746	-115.3825	517.84	37.38	13.85	13.27	-62.3034	470.6778	44.30	10.62	9.96	-62.3034	301.88	44.3	6.81	5.87
22	1066	PBCHM69534497	-73.1952	228.86	37.49	6.10	25.29	-115.5157	941.9600	66.07	14.26	75.87	-115.5157	539.16	66.07	8.16	43.42
23	1070	ZINC20381469	-75.4117	486.55	36.74	13.24	45.09	-119.6377	224.9200	48.8	4.61	27.64	-119.6377	267.67	48.8	5.49	32.89
24	1072	PBCHM11746172	-115.5157	175.32	37.89	4.63	5.06	-57.8986	164.9560	54.11	3.05	2.78	-57.8986	299.41	54.11	5.53	4.93
25	1077	PBCHM2782232	-62.2768	558.64	37.69	14.82	10.13	-62.7087	6534.5500	53.55	122.03	62.48	-62.7087	1471.51	53.55	27.48	14.07
26	1083	PBCHM81560982	-57.8986	333.39	37.10	8.99	38.31	-75.4106	244.3820	55.9	4.37	30.79	-75.4106	-123.65	55.9	-2.21	-10.15
27	1088	PBCHM2732702	-75.4106	237.21	37.76	6.28	26.16	-116.8663	625.4300	45.83	13.65	44.72	-116.8663	606.47	45.83	13.23	43.37



Table 2 Six new hit compounds from the hit expansion competition assay

Library Entry	location	Seed compound public ID	Analogue public ID	Chemical structure	Height reduction	Noise	Reduction/ noise	Height decrease (%)
1	1009	CHEMBL1673279	PBCHM45210798		153.86	37.44	4.11	8.74
2	1048	PBCHM3049683	PBCHM57223647		167.81	37.10	4.52	2.96
3			ZINC00159801		130.88	37.44	3.50	2.32
4			ZINC00057047		75.89	37.48	2.02	1.32
5	1055	PBCHM120765	CHEMBL448523		298.75	36.90	8.10	5.91
6			ZINC00120199		159.16	36.94	4.31	1.63

NMR screening were prepared from synthetic A $\beta_{1-42}$  polypeptide using a protocol previously described.<sup>37,38</sup> Briefly, dry films were prepared from hexafluoro-2-propanol (HFIP) solution of synthetic A $\beta_{1-42}$  polypeptide which were then hydrated with Neurobasal medium and desalted using a HiTrap column. The fractions collected with known A $\beta_{1-42}$  monomer concentrations were allowed to oligomerize for 1 hour at room temperature, followed by centrifugation. The supernatant containing A $\beta$  were collected and characterised by dynamic light scattering (DLS) technique. The size and distribution of amyloid beta (A $\beta_{1-42}$ )-derived diffusible ligand (ADDL) preparations were assessed (Fig. 2a). A typical profile of the A $\beta$  preparation consisted of three major populations of oligomers with hydrodynamic radii between 10 nm and 100 nm (Fig. 2b). This size distribution profile is broadly in line with the A $\beta$  isolated from human brain tissues of AD patients.<sup>39</sup> Despite the fact the formation of oligomers and fibrils are dynamic in nature, the oligomers prepared using this protocol showed about 70% oligomer population as smaller species with an average molecular weight of 146 kD. Given that the molecular weight for A $\beta_{1-42}$  monomer is at around 4.5 kD, Most oligomers should exist as 30-mers or below which falls in the range of 10–50-mers soluble A $\beta$  that exist natively in the brain of AD patients.<sup>40</sup> The A $\beta$  prepared maintains good solubility in buffers used in NMR experiment as the oligomers up to 1600-mers were reported in a soluble state.<sup>41</sup> Due to the large quantity and high purity of A $\beta$  required for NMR screening, it is not viable and ethical to extract them from human AD brain tissue, we adapted a protocol to produce A $\beta$  from synthetic A $\beta_{1-42}$  monomers that resemble the native A $\beta$  population as much as possible despite of heterogeneity of the

distribution. The A $\beta$  of this profile were used for all NMR experiments in this paper unless otherwise stated.

**Design and validation of NMR screening techniques.** To assess the suitability of the A $\beta$  prepared for the NMR screening experiments and optimize the assay conditions, bexarotene was selected to validate the binding interaction between A $\beta$ -oligomers and small molecules. Bexarotene is a clinically proven anticancer treatment for cutaneous T cell lymphoma (CTCL)

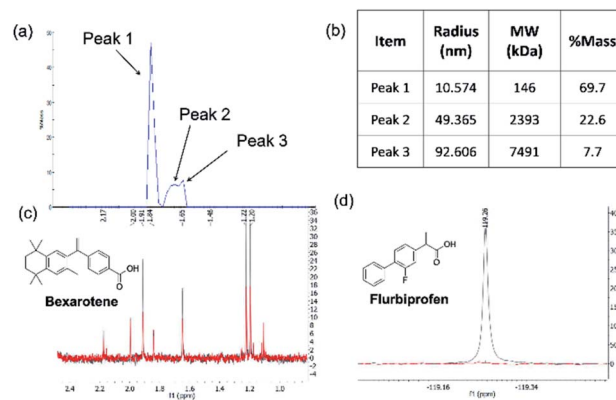


Fig. 2 A $\beta_{1-42}$  oligomer preparation and validation of NMR protocols. (a) size exclusion profile of the preparation over 1 hour (b) size of the oligomers analysed by dynamic light scattering (DLS) technique; (c) Section of  $^1\text{H}$  NMR spectra of 50  $\mu\text{M}$  bexarotene in the presence (red) and absence (blue) of 1  $\mu\text{M}$  of A $\beta$ . The reduction of peak height upon the addition of the A $\beta_{1-42}$  oligomer preparation indicates an interaction between bexarotene and the oligomer preparation; (d) section of  $^{19}\text{F}$  NMR spectra of 50  $\mu\text{M}$  flurbiprofen in the presence (blue) and absence (red) of 1  $\mu\text{M}$  of bovine serum albumin (BSA).



and off-label treatment for lung and breast cancers.<sup>42–44</sup> It was reported to compete with cholesterol in A $\beta$  binding and inhibit the amyloid aggregation.<sup>45–48</sup> Because there was no fluorinated bexarotene available, <sup>1</sup>H-CPMG NMR experiments were used in the binding assay. The overlay of the spectra of bexarotene in the presence and absence of A $\beta$  is presented in Fig. 2c. The reduction of peak height in the presence of the oligomers in this experiment confirms the binding between bexarotene and A $\beta$  prepared. Bexarotene was therefore selected as a positive control in all relevant NMR experiments unless otherwise stated.

The same protocol was applied to a model system to test if the experimental conditions for bexarotene and A $\beta$  were applicable for <sup>19</sup>F NMR screening of virtual hits from computer modelling. A model system consisting of bovine serum albumin (BSA) and its known fluorine-containing binding ligand, flurbiprofen, was constructed. The flurbiprofen is a nonsteroidal anti-inflammatory agent (NSAIA) with antipyretic and analgesic activity. It is an analogue of ibuprofen and >99% of it was bound to albumin after administration.<sup>49,50</sup> Suppression of the <sup>19</sup>F signals (Fig. 2d) of flurbiprofen upon BSA binding clearly demonstrated that the <sup>19</sup>F NMR protocol can be used as a primary screening tool for virtual hits against A $\beta$  prepared.

<sup>19</sup>F CPMG NMR is becoming an increasingly popular tool in the field of drug screening<sup>51</sup> because each <sup>19</sup>F atom, which is a 100% naturally abundant fluorine NMR-visible isotope, is absent in biomolecules such as proteins, F-containing compounds generates a unique chemical shift in the spectrum which is often simple with no erroneous background noise and interference from other signals, and hence can be easily identified.<sup>52</sup> Moreover the fluorine nucleus is very sensitive to changes in the chemical environment, and can be a very sensitive probe even for the weakest binders. In addition, the large chemical shift range and the strong chemical shift anisotropy make it very simple to measure mixtures of up to 30 fragments in a single sample. When a small molecule is bound to a large protein, the signal intensity of the binding ligand is significantly attenuated by Carr–Purcell–Meiboom–Gill (CPMG) or spin-lock pulse due to interaction with protein. In this experiment, the <sup>19</sup>F NMR methodology provides a sensitive tool not only for probing compound binding to A $\beta$ , but also for rapidly deconvoluting library members from the mixture due to the unique shift of each library member in <sup>19</sup>F NMR spectra.<sup>53</sup> Therefore, the throughput of the NMR screening can be increased and the amount of A $\beta$  required for the screening reduced. The only disadvantage of this technique is that compounds tested (in direct binding measurement at least) need to have at least one fluorine atom.

**Primary screening by <sup>19</sup>F-CPMG NMR.** In this work, a collection of 971 fluorine-containing hits from the virtual screen were sourced for <sup>19</sup>F CPMG NMR screening from Lilly's internal compound collection. These compounds were initially tested for their solubility and stability in the media which was used for the A $\beta$  oligomer preparation in the method validation section. Compounds that were not suitable were discarded and individual <sup>19</sup>F CPMG NMR spectrum for each of the remaining 614 compounds were acquired and stored for compound

grouping in sub-library design and for hit identification. These 614 compounds were then organised into 91 sub-libraries, each containing 6 or 7 compounds. The sub-libraries were designed using a modified version of the NMRmix software and based on individual chemical shifts of each compound in the <sup>19</sup>F-CPMG NMR spectrum. The chemical shift(s) of each compound in the library were spread out as far as possible, yet not exceeded a spectral width causing pulses in the sequence to deviate significantly from the ideal. Compounds with overlapping chemical shifts were placed in different libraries. The sub-libraries were also designed to ensure that chemical shifts from library members are sufficiently different to allow immediate assignment of any active components.

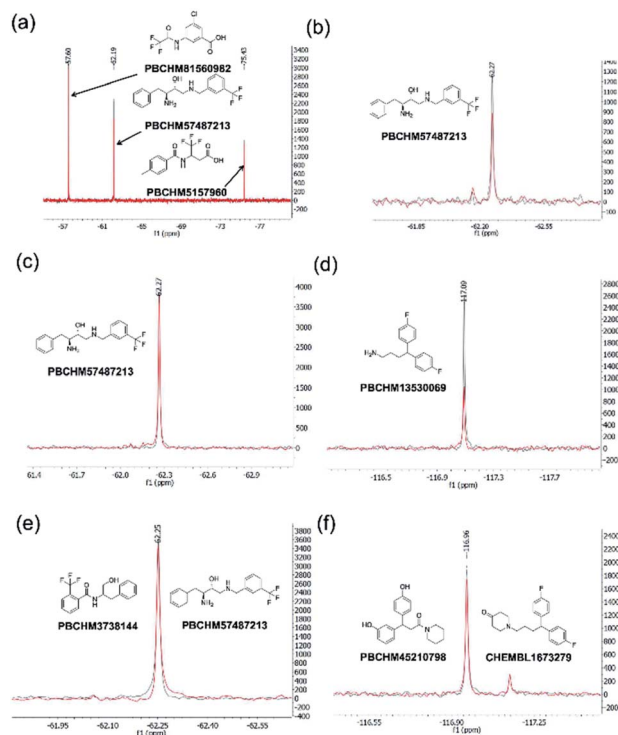


**Fig. 3** <sup>19</sup>F CPMG NMR screening. (a) Section <sup>19</sup>F CPMG NMR spectra of sub-library 1045 containing 50  $\mu$ M of compound ZINC02382246 (–57.6 ppm), PBCHM57487213 (–62.3 ppm) and PBCHM5157960 (–75.5 ppm) in the presence (red) and absence (blue) of 1  $\mu$ M (concentration as monomer) A $\beta$ ; (b) section <sup>19</sup>F CPMG NMR spectra of PBCHM57487213 (–62.3 ppm) in the presence (red) and absence (blue) of 1  $\mu$ M (concentration as monomer) A $\beta$  in the individual <sup>19</sup>F NMR confirmation run; (c) section <sup>19</sup>F CPMG NMR spectra of PBCHM57487213 (–62.3 ppm) in the presence (red) and absence (blue) of 1  $\mu$ M (concentration as monomer) scrambled peptide; (d) section <sup>19</sup>F CPMG NMR spectra of PBCHM13530069 (–62.3 ppm) in the presence (red) and absence (blue) of 1  $\mu$ M (concentration as monomer) scrambled peptide; (e) <sup>19</sup>F CPMG NMR spectra of 50  $\mu$ M of seed compound PBCHM57487213 binding to 1  $\mu$ M (concentration as monomer) A $\beta$  in competition with 50  $\mu$ M of analogue PBCHM3738144 in the presence (red) and absence (blue) of the analogue compound in the hit expansion experiment; (f) <sup>19</sup>F CPMG NMR spectra of 50  $\mu$ M of seed compound CHEMBL1673279 binding to 1  $\mu$ M (concentration as monomer) A $\beta$  in competition with 50  $\mu$ M of analogue PBCHM45210798 in the presence (red) and absence the analogue compound in the hit expansion experiment.



The  $^{19}\text{F}$  CPMG NMR experimental protocol described above was then used to screen compounds in 91 fluorine-containing sub-libraries in the presence and absence of  $\text{A}\beta$ . An example of sub-library screening is illustrated in Fig. 3. A section of spectra of three compounds from the  $^{19}\text{F}$  CPMG NMR experiment of sub-library mixture 1045 containing six compounds in the absence (blue) and the presence (red) of  $\text{A}\beta$  is shown in Fig. 3a. It was seen that compound **PBCHM57487213** showed a noticeable reduction in the peak height.

In order to assess if any changes in peak intensity are statistically significant, the ratio of peak reduction/noise and % of peak height reduction are calculated for each compound. The ratio of peak reduction/noise represents the significance of the peak reduction in reference to the base-line noise. A ratio of  $>2$  has been assigned as the cut-off for a positive hit. The larger the ratio, the more reliable the data is. The percent peak reduction gives an indication of the relative binding abilities of compounds in each sub-library, therefore was used as a key parameter for measuring binding strength.

For each compound, hit compound entry, its sub-library number where it was tested, public ID, chemical shift, reduction in the peak height upon binding to  $\text{A}\beta$ , baseline noise, signal reduction/noise ratio as well as percent of peak height reduction compared to the peak height in the absence of  $\text{A}\beta$  are collected, presented and analysed. The 27 compounds that showed positive responses in the presence of  $\text{A}\beta$  are shown under  $^{19}\text{F}$  NMR sublibrary screening column in Table 1.

It can be seen that 27 hit compounds came from 24 sub-libraries and displayed a spectrum of abilities in peak height reduction. Judged by % of peak height reduction, four compounds (Table 1, entries 4, 18, 23 and 26) produced over 30% reduction in peak height, hence are classified as strong binders. 3 compounds (Table 1, entries 2, 22, and 27) reduced peak height by over 20%, hence are classified as medium binders. The rest of the compounds gave between 5 and 16% reduction in peak height in the presence of  $\text{A}\beta$  making them weak binders. Although the binding ability is arbitrarily assigned, it provides a tool for ranking the binding significance of the compounds. It is tempting to conclude stronger binders generally display a bigger ratio of peak reduction/noise than weaker binders: fraction bound will indeed be one component of the response, but other factors may also be important, so too much significance should not be placed on this. The chemical structures for all 27 hit compounds with their public IDs are shown in Fig. 4.

To remove false positives caused by compound–compound interactions, compounds which were active within the mixture screen were re-tested *via* the  $^{19}\text{F}$  CPMG NMR experiment individually under the same conditions as they were screened in the library mixtures and a sample is shown in Fig. 3b. Using the same criteria and cut-offs applied in the primary sub-library screening, 24 out of 27 compounds showed reductions in the peak height in the presence of  $\text{A}\beta$  in the individual binding experiments, hence were deemed to be confirmed hit binders (under  $^{19}\text{F}$  NMR individual experiment column Table 1). It is interesting to observe that the binding of most compounds (Table 1, entries 1, 4, 10, 13, 14, 15, 21, 24 and 26) to  $\text{A}\beta$  in the

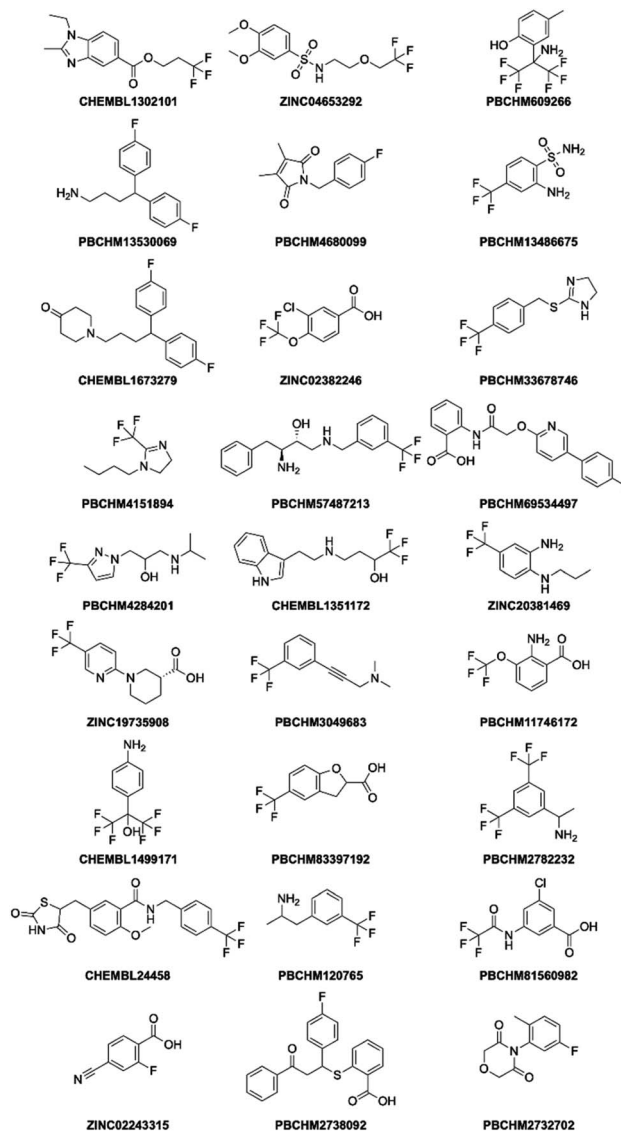


Fig. 4 Structure of 27 hits from sub-library screening.

individual confirmation experiment remained at a similar level as displayed in the primary sub-library screening. This demonstrates that the binding of these compounds was not affected by other compounds present in the library. Compound entries 2, 3, 7, 8, 13, 18, 19, 20 and 27 showed noticeable increases ( $>50\%$ ) in the % peak height reduction, when compared with the reduction seen in the sublibrary screening, showing that presence of other compounds in the sub-library inhibits their binding to  $\text{A}\beta$ . Compound entries 5, 11, 16, 17, 21, and 23 displayed significant reduction in the % peak height reduction when compared with the reduction seen in the sub-library screening, showing that the presence of other compounds in the sub-library enhances their binding to  $\text{A}\beta$ .

It is worth mentioning that compound entries 10 and 11, belong to the same sub-library (Library 1043), but behave differently in the individual experiments. The presence of compound entry 10 seems to enhance the binding of compound



entry 11 to A $\beta$  while the presence of compound entry 11 does not seem to affect the binding of compound entry 10. However, the interference of other compounds in the sub-library cannot be completely ruled out. Compound entries 12 and 13 (Library 1045) displayed the opposite influence of one compound to the other when compared with compound entries 10 and 11. Compound entries 17 and 18 (Library 1055) affected each other significantly when present in the sub-library mixture. The presence of compound entry 17 significantly inhibits the binding of compound entry 18 to A $\beta$  in the sub-library while the presence of compound entry 18 significantly enhances the binding of compound entry 17. This shows that they not only bind to A $\beta$  individually, but also together they exhibit the strongest effects of compound–compound interaction upon the binding compared with the other two pairs. Three compounds (Table 1, entries 6, 9 and 12) displayed a negligible reduction in peak height when re-tested individually. This shows their bindings to A $\beta$  rely on their interaction with other compounds in the corresponding sub-libraries. It may also mean that they are interacting with each other. Ligand–ligand interactions cannot be ruled out either.

The number of compounds which belong to strong binders increased from 4 to 11 and the % of peak reduction of some compounds has even doubled (Table 1, entries 2, 8, 19, 20, 22 and 25). The number of compounds in the medium-binder category increased by 1 and the number of weak binders reduced by 8. 3 compounds (Table 1, entries 6, 9 and 12) became non-binders and were removed from the hit list.

To avoid false positives arising from non-specific binding, these 27 initial hits were also subjected to a counter screen against a scrambled (non-amyloid) peptide which has the same amino acid composition and peptide chain length, but a different primary sequence to A $\beta_{1-42}$ . The scramble was prepared using the same protocol as that of A $\beta$  from A $\beta_{1-42}$ .

A counter screen of each compound against a scrambled peptide was also carried out in individual experiments using the same  $^{19}\text{F}$  CPMG NMR technique. The scrambled peptide possesses the same composition of amino acids, but different primary sequence as that of disease-causing A $\beta_{1-42}$  sequence. It does not aggregate to form amyloid fibrils, therefore is often used as a control peptide to examine the specificity for A $\beta$  binders. The scrambled peptide was subjected to the same preparation protocol as that of A $\beta$  prepared from synthetic A $\beta_{1-42}$  monomers. The binding between the hit compounds and the scrambled peptide was performed using the same protocol as the one used for A $\beta$  binding.

All 27 initial  $^{19}\text{F}$  NMR sub-library hits (including the 3 negative hits in the individual confirmation experiment) were tested against the scrambled peptide and data is displayed in the “ $^{19}\text{F}$  NMR scrambled peptide experiment” column in Table 1. An example of spectra for compound **PBCHM57487213** (Table 1, entry 13) in the absence (blue) and presence (red) of scramble peptides are shown (Fig. 3c). No change in the peak height reduction was observed demonstrating that it does not bind to the scrambled peptide, hence is a specific binder for A $\beta$ . An example of non-specific A $\beta$  binder can be seen with compound **PBCHM13530069** (Table 1, entry 2). This compound a positive

hit in the initial sub-library screening as well as the individual confirmation  $^{19}\text{F}$ -CPMG NMR screening (Fig. 3d). However, it showed significant binding to the scramble peptide, hence is removed from the list of compounds for further investigation.

Out of 27 compounds, 11 were identified as specific A $\beta$  binders that have a ratio of peak height reduction/noise less than 2 in the presence of scrambled peptide with negative or small % of peak height reduction. Compound entries 9 and 12, having already shown to be non-binders in the individual NMR experiment, also displayed no binding to the scrambled peptide. Notably, compound entry 6, also a non-binder in the individual experiment, displayed significant binding to the scrambled peptide. A compound can only be classified as a hit if they showed peak height reduction in both sub-library screening, individual experiment, and no peak reduction in the scrambled peptide experiment. Hence, compound entry 6 was also removed from the hit list. This leaves 8 confirmed hits in total (Table 1, entries 3, 7, 11, 13, 14, 15, 17, 26).

From the initial 614 compound library to 8 confirmed hits, a hit rate of 1.3% was obtained which is higher than average random high throughput campaign hit rate (0.01% and 0.14%).<sup>54</sup> These hits were taken forward to the hit expansion experiment.

**Screening of hit expansion analogues.** Utilising a fingerprint similarity method, 36 near neighbour analogues of the 8 F-containing hit compounds were identified from the original database of 73 848 compounds. These compounds are non-proprietary, commercially available and were in stock in the Lilly inventory.

The 36 analogues were screened against their respective “seed/parent compounds” in a competition experiment using  $^{19}\text{F}$  NMR technique employed in the primary screening to rapidly acquire data and compound deconvolution.<sup>55</sup> A solution was prepared containing the same concentration of the seed compound and its corresponding analogue, and the change in peak height of the original F-containing seed compound in the presence of its analogue and A $\beta$  was analysed. If the original seed compound still displayed a reduction of peak height twice that of the noise in the presence of the structural analogue, it was deemed that the analogue displayed specific binding to the same location as the seed compound. In the competition experiment between seed compound **PBCHM57487213** and its near neighbour analogue **PBCHM3738144**, it is clear that there is no competition between the compounds as no peak height reduction is observed (Fig. 3e). This indicated that the analogue **PBCHM3738144** is either a weaker binder than its seed compound **PBCHM57487213** or it binds to a different site from where its seed compound binds and does not interrupt the binding of the seed compound. Conversely, analogue **PBCHM45210798** clearly competes with its seed compound **CHEMBL1673279** (Fig. 3f) suggesting that this analogue binds at the same site on A $\beta$  as its seed compound. Its binding strength is strong enough to compete its seed compound partially off. From the expansion competition experiment, 6 out of 36 compounds were identified as potential binders. Their original location, seed compound public ID, analogue public ID, chemical structure, NMR data on competition assay (peak



height reduction, noise, reduction/noise ratio, % peak height reduction) are shown in Table 2.

Although this competition experiment would suggest competitive binding between the analogue and the seed for the same site on A $\beta$  it does not eliminate the potential for the analogues to allosterically inhibit the seed compound. From this expansion experiment, 6 further hit compounds were identified as potential binders (Table 2) giving a total of 14 hit compounds from the  $^{19}\text{F}$  CPMG NMR experiments described above. The hit rate has increased by 13-fold, from 1.3% in the primary screening to 17% in the hit expansion exercise. This hit rate enhancement demonstrates the viabilities of both the computational and NMR approaches.

### Characterisation of the binding using saturation transfer difference (STD) NMR

To further validate the hit compounds obtained from the initial  $^{19}\text{F}$  NMR screening, a STD screen was used as an orthogonal binding study to characterise binding affinity and identify hot spots on the molecule that are involved in the binding.<sup>56</sup>

Saturation Transfer Difference (STD)-NMR is often employed during the drug discovery process as a method of binding validation which is complementary to  $^{19}\text{F}$  NMR screening. STD NMR is increasingly used as a semi-quantitative method for epitope mapping on ligand moieties interacting with the protein.<sup>57</sup> An STD NMR experiment starts with the selective irradiation of the protons of the large biomolecule, such as a protein, using Gaussian  $R_f$  pulses. The resulting  $R_f$  saturation is then rapidly propagated across the entire protein through a spin diffusion effect *via* non-scalar magnetization transfer. If a smaller molecule ligand binds the receptor, saturation will also spread onto the ligand. As a result, intensity of the proton signals on the ligand will be attenuated. Subtraction of resulting spectrum from a reference spectrum without saturation yields the STD spectrum containing only signals of the binding ligand.<sup>56</sup> STD NMR can be used to characterise weak ligand binding ( $K_d \sim \text{mM}$  to  $\mu\text{M}$ ) and map the hot spots on the ligand that are involved in the binding to large protein molecules ( $M_w > 20$  kDa).<sup>57</sup> It does not require expensive stable isotopes or radioisotope labelling and only requires small amount of protein (nM to pM), hence is an economical method to analyse protein–ligand interactions especially when a large quantity of the protein under study is not achievable. During the experiment, the small molecules are usually used in large excess (20–1000 times excess) of the protein concentration.

The STD-NMR protocol used in the current study was verified by using two model systems: BSA and its known small ligand binder, Iburpofen (Fig. 5a), and A $\beta$  and bexarotene (Fig. 5b). Examples of STD NMR spectra of two hit compounds are shown in Fig. 5c and d.

In each of the model systems, the STD NMR experiment produces a “difference” spectrum by subtracting two contrasting “saturation” spectra. The first NMR spectra recorded is an off-resonance saturation (no protein saturation ‘STD<sub>off</sub>’) spectra where the excitation pulse is away from the protein  $^1\text{H}$  signal. This STD<sub>off</sub> spectra is referred to as the “reference” spectra as it

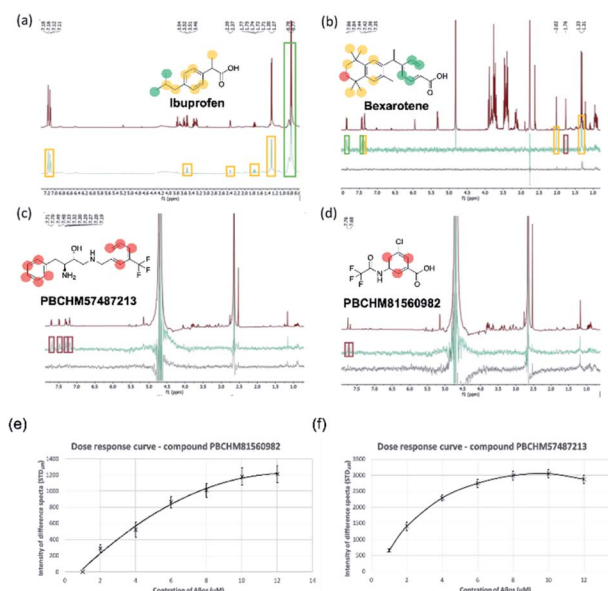


Fig. 5 STD NMR characteristics (a) section of an STD spectra of 200  $\mu\text{M}$  ibuprofen and 2  $\mu\text{M}$  of bovine serum albumin (BSA) containing a glucose (200  $\mu\text{M}$ ) control. Reference spectra (grey) and on-resonance spectra (black); (b) section of an STD spectra of 200  $\mu\text{M}$  bexarotene and 2  $\mu\text{M}$  (concentration as monomer) A $\beta$ . Reference spectra (red), on-resonance spectra (green), control (black). (c) STD NMR of 200  $\mu\text{M}$  of PBCHM57487213 and 2  $\mu\text{M}$  (concentration as monomer) A $\beta$ . (d) STD NMR of 200  $\mu\text{M}$  of compounds PBCHM81560982 and 2  $\mu\text{M}$  (concentration as monomer) A $\beta$ . Reference (red) spectra, on-resonance spectra (green), control (black). Color scheme on the structure: ranges of values for %STD moiety analysis: red =  $\leq 5\%$ , yellow =  $\geq 10\%$ , green =  $> 10\%$ . (e) Dose response curve – compound PBCHM57487213; (f) dose response curve – compound PBCHM81560982.

is comparable with a standard  $^1\text{H}$ -NMR spectrum of the ligand (Fig. 5a (grey), Fig. 5b–d (red)). The second NMR spectra is an on-resonance saturation (selective protein proton saturation ‘STD<sub>on</sub>’) spectra where the excitation pulse is directed at a known protein  $^1\text{H}$  signal and does not interact directly with the added ligand. This STD<sub>on</sub> spectra displays decreases in peak intensity for the bound ligands. This is due to the transfer of energy from the excited protein to the ligands in closest proximity *via* the proton network. The difference spectra (STD<sub>diff</sub>) is the subtraction of the STD<sub>off</sub> spectra from the STD<sub>on</sub> (STD<sub>diff</sub> = STD<sub>off</sub> – STD<sub>on</sub>) (Fig. 5a (black), Fig. 5b–d (green)). The STD<sub>diff</sub> highlights the small changes in peak height from the STD<sub>off</sub> to the STD<sub>on</sub> that are not identifiable.

Finally, to eliminate potential ligand–ligand interactions interfering with the experiment the same excitation pulses and STD<sub>diff</sub> were recorded without the presence of a protein and referred to as a “control” (Fig. 5b–d (black)). If a response was seen in the “control” it was believed to be due to ligand–ligand interactions and this false positive discarded.

From the STD-NMR experiment, additional information on the closest proximity proton functionalities ‘hot spots’ on each of the compound moieties can be measured semi-quantitatively from the magnitude of the STD effect. The STD effect can be





represented numerically as a percentage ( $(\text{STD}_{\text{diff}} \text{ integral} / \text{STD}_{\text{off}} \text{ integral}) \times 100$ ). For each of the binders, a maximum STD effect of each moiety was calculated and mapped onto the atoms in each compound. The level of the STD effect was then mapped onto the atoms of each compound and colour-coded to reflect the semi quantitative nature of the technique.

The binding between BSA and ibuprofen, with non-binding spy compound glucose present, is shown in Fig. 5a. In the  $\text{STD}_{\text{off}}$  spectrum, chemical shifts for glucose can be seen between 3 and 4 ppm which are not presented in the  $\text{STD}_{\text{diff}}$  as glucose is not involved in the binding (Fig. 5a). The atoms on the ibuprofen that are involved in the binding to BSA and their level of commitments (% difference) in the binding are labelled and colour-coded in the  $\text{STD}_{\text{diff}}$ . It is clear that the carboxylic acid group should have the strongest interactions with BSA as BSA is the most abundant hydrophilic globular protein in blood serum acting primarily as a carrier protein for hormones, fatty acids, trace minerals, vitamins and iron.<sup>58</sup> Strong interactions between BSA and ibuprofen involve the aromatic region and connected sidechains. This is expected because there are hydrophobic side chains and peptide backbones in BSA which favour hydrophobic interactions. This study complements to the molecular interactions identified through the X-ray studies of co-crystallisation of BSA and ibuprofen where hydrophobic part of the molecule interacts strongly with the binding pocket around Val349A and carboxylic acid group forms hydrogen bonds with Tyr355A and Arg120A.<sup>59,60</sup>

In the more relevant model system, atoms involved in the binding between A $\beta$  and bexarotene are labelled and colour-coded in the  $\text{STD}_{\text{diff}}$  spectrum ( $\text{STD}_{\text{off}}$  Fig. 5b (red)), ( $\text{STD}_{\text{diff}}$  Fig. 5b (green)) and ( $\text{STD}_{\text{control}}$  Fig. 5b (black)). As expected, A $\beta$  are hydrophobic in nature, it is therefore not surprising to see the interactions heavily rely on the hydrophobic part of the molecule. The involvement of the carboxylic acid group cannot be defined from the STD experiment although some ionic interactions between the group and amine side chains should play roles in driving the initial interaction or enhancing/stabilising the interaction.

The protocols developed were applied to study the binding between A $\beta$  and our hit compounds from the  $^{19}\text{F}$  NMR screen (Fig. 5c and d).  $\text{STD}_{\text{off}}$ , (red),  $\text{STD}_{\text{diff}}$  (green) and control (black) spectra were recorded for **PBCHM57487213** and **PBCHM81560982**. Atoms involved in the binding between A $\beta$  and the ligands are labelled and color-coded in the  $\text{STD}_{\text{diff}}$  spectra. Both compounds were shown to be medium to strong binders in the sub-library screening and individual confirmation  $^{19}\text{F}$  NMR experiments. Additionally, they were confirmed specific binders from the scrambled peptide screening. Although the percent peak differences are small and the involvement of non-hydrogen atoms cannot be confirmed, the aromatic protons are all shown to be affected upon A $\beta$  binding just like bexarotene in this STD NMR experiment. This again demonstrates that the  $\pi$ - $\pi$  and hydrophobic interactions are important in this type of molecular interactions.

The STD-NMR experiment was carried out with each of the 14 hit compounds with the addition of A $\beta$ . Of the 8 initial hit compounds from the first round of screening, 7 of them were

Table 3 Summary of STD NMR data on 14 confirmed hit compounds from  $^{19}\text{F}$  NMR experiments

Entry	Public ID	Analogue public ID	Structure	Highest% STD
1	<b>CHEMBL1673279</b>			4.31
2		<b>PBCHM45210798</b>		15.51
3	<b>CHEMBL1499171</b>			0.00
4	<b>PBCHM4680099</b>			7.40
5	<b>PBCHM57487213</b>			0.89
6	<b>CHEMBL1351172</b>			2.77
7	<b>PBCHM3049683</b>			6.02
8		<b>PBCHM57223647</b>		0.00
9		<b>ZINC00159801</b>		0.00
10		<b>ZINC00057047</b>		0.00
11	<b>PBCHM120765</b>			8.07
12		<b>CHEMBL448523</b>		0.00
13		<b>ZINC00120199</b>		8.13
14	<b>PBCHM81560982</b>			0.75
15	Bexarotene			14.60

confirmed binders by STD NMR experiments (Table 3). Compound **CHEMBL1499171** showed no change of signal in the STD NMR experiment, and was thus deemed inactive. Compared to other hit binders, it was noted that this molecule is smaller than the others (Fig. 4). We might speculate that this smaller fragment is either of lower affinity or makes less contacts with the protein, both of these would result in a weaker STD signal. There is no direct correlation between  $^{19}\text{F}$  NMR signal strength and STD-NMR signal change for any of the compounds.

Only 2 out of the 6 compounds from the hit expansion experiment showed noticeable changes in STD-NMR signals. It is interesting to note that none of the 3 analogues from the



same seed-compound, **PBCHM3049683**, showed any changes in STD signals while the parent compound itself showed a good response. As above, it is noted that the smaller more fragment-like molecules give weaker STD signals, which may be due to weaker binding or less efficient contacts with the protein. This could indicate that competition assay alone may not be the best method used for hit identification. Other validation assays such as STD NMR should be used together to confirm the hits. Of course, it can also indicate that STD NMR is not the best technique to pick up small molecular weight binders. It is interesting to note that hit compound **CHEMBL1673279** and its analogue **PBCHM45210798** consistently showed good binding abilities in all  $^{19}\text{F}$  NMR and STD NMR experiments. The same trend is seen with hit compound **PBCHM120765** and its analogue **ZINC00120199**. 14 hit compounds from  $^{19}\text{F}$  CPMG NMR techniques were subject to the STD filter and 9 compounds were confirmed as binders from STD NMR experiments (Table 3).

Compounds **PBCHM57487213** and **PBCHM81560982** were chosen for dose response studies (Fig. 5e and f). As STD NMR experiments are performed in an excess of ligand, in order to measure a dose–response curve, the concentration of the ligand was kept consistent while the concentration of  $\text{A}\beta$  was incrementally increased. The spectra were acquired over the same period of time and the integral of the  $\text{STD}_{\text{diff}}$  was measured. Both compounds adhere to a standard response of increased protein concentration. Initially, there is an increase in response as the protein concentration is increased and the curve then begins to plateau indicating the active sites of the proteins are completely occupied and this is the maximum response for the STD experiment. Finally, the curve began to decrease as the ligand and protein will no longer be in fast exchange. This decreases the response of the STD experiment. The estimated  $K_{\text{d}}$  for compound **PBCHM57487213** is  $\sim 2 \mu\text{M}$  and compound **PBCHM81560982** is  $4 \mu\text{M}$ . The dose response for other STD NMR confirmed hits were not carried out due to the availability of those compounds.

From the 9 potential binders identified from the  $^{19}\text{F}$  CPMG and STD-NMR experiments, 6 compounds (**CHEMBL1673279**, **PBCHM4680099**, **PBCHM57487213**, **ZINC00120199**, **PBCHM120765**, and **PBCHM81560982**) were chosen to be taken forward and tested in a biological assay to assess the effect of their binding upon the interfere the binding between  $\text{A}\beta$  and  $\text{PrP}^{\text{C}}$ , and their effects on Fyn and Tau. These compounds were chosen due to their structural diversity, biophysical results and availabilities.

### Biological and functional evaluation of selected hit compounds

To further evaluate the compounds that we identified in the biochemical assay, we sought to answer the following questions: (1) if  $\text{A}\beta$  prepared interacts with  $\text{PrP}^{\text{C}}$  as previously reported;<sup>11,61</sup> (2) if the  $\text{A}\beta$  binders identified from NMR screening interfere with  $\text{A}\beta$ – $\text{PrP}^{\text{C}}$  binding in a biologically relevant manner; (3) if so, do they have polypharmacological properties, *i.e.* any effects on downstream signalling (pFYN and pTau

activities). In order to address these issues, different cellular screening models were developed.

**The hit  $\text{A}\beta$ -binders disrupt interactions between  $\text{A}\beta$  and  $\text{PrP}^{\text{C}}$  on HEK293 cells.** First of all, a cellular model was developed to assess the binding between the  $\text{A}\beta$  preparation and  $\text{PrP}^{\text{C}}$  on the cell surface. For this, four different human cell lines of both neuronal and non-neuronal origins were tested. A wild type HEK293 cell line derived from human embryonic kidney cells which was previously reported for studying  $\text{A}\beta$ – $\text{PrP}^{\text{C}}$  binding.<sup>62</sup> iCells which are human glutamatergic-enriched cortical neurons derived from iPSC and two SH-SY5Y cell lines which were sub-cloned from a bone marrow biopsy derived line expressing neuron-like characteristics.

We examined the level of PRNP and other Alzheimer's disease related genes in each cell line, including FYN, NMDA receptor genes (GRIN1, GRIN2A, GRIN2B), mGluR5 (GRM5), NACE1 and Tau producing gene (MAPT) (Fig. 6a). We found that iCells showed the greatest expression of all examined genes while SH-SY5Y cells contain the least relevant genes, PRNP gene in particular. However, the wild type HEK293 cell line was selected for studying  $\text{A}\beta$  and  $\text{PrP}^{\text{C}}$  binding because it had moderate expression of the studied genes and it is also a robust cell line, easy to maintain at low cost, and amenable for high throughput screening. The expression of  $\text{PrP}^{\text{C}}$  protein in the HEK293 cell line is visualised by staining against anti- $\text{PrP}^{\text{C}}$  antibody 8H4 (Fig. 6b) confirmed and quantified by flow cytometry (Fig. 6c).

With the HEK293 cell line being selected as a cellular model for direct binding studies, the  $\text{A}\beta$  preparation used in the NMR screening was tested for their binding to  $\text{PrP}^{\text{C}}$  on the surface of HEK293 cells. The cells were stained by anti- $\text{A}\beta$  antibodies, Phalloidin (cytoskeleton stain) and DAPI (nuclei). Both synthetic  $\text{A}\beta_{1-42}$  oligomers as described above and recombinant  $\text{A}\beta$  produced by CHO 7PA2 cells were examined in the binding studies to  $\text{PrP}^{\text{C}}$  in the HEK293 cell model and both showed similar level bindings (data not shown). However,  $\text{A}\beta$  prepared from synthetic  $\text{A}\beta_{1-42}$  monomers displayed noticeable interference in immunostaining in confocal and ICC assays due to some large particles present which did not pose much problems in NMR experiments. The recombinant  $\text{A}\beta$  were obtained from the supernatant after harvest of the cells and debris removed. They contain a heterogeneous population of monomers, dimers, trimers, tetramers, higher state soluble oligomers and other cellular proteins as previously reported by western blotting. The recombinant  $\text{A}\beta$  were therefore used in all cellular assays (HEK cell binding assay and subsequent hiPSC functional assays). The recombinant  $\text{A}\beta$  were produced by CHO 7PA2 cells transfected with cDNA encoding APP751 containing Val 717Phe familial AD mutation and quantified by ELISA.

When compared with the control (Fig. 6d, first panel),  $\text{A}\beta$  were shown to be able to bind to  $\text{PrP}^{\text{C}}$  on the cell surface of HEK293 cells (Fig. 6d, second panel). The binding of  $\text{A}\beta$ – $\text{PrP}^{\text{C}}$  can be significantly blocked by anti-prion antibody 6D11, raised against the epitope containing amino acids 93–109 of  $\text{PrP}^{\text{C}}$ . This antibody was reported to block the interaction between  $\text{A}\beta$  and  $\text{PrP}^{\text{C}}$ .<sup>61,63</sup> Its inhibitory effect was confirmed in our HEK293 direct binding assay (Fig. 6d, third panel). The inhibition of



6D11 on the binding of A $\beta$  to PrP<sup>C</sup> on the cell surface was further reduced by PLC treatment as previously reported<sup>64</sup> (Fig. 6d, forth panel). The binding of A $\beta$  on endogenous PrP<sup>C</sup> on wild type HEK293 cells and inhibitory effect of known inhibitors, 6D11 and PLC are quantified (Fig. 6e).

The ability of our hit compounds to disrupt the A $\beta$ -PrP<sup>C</sup> interaction in HEK293 cells was assessed using a live-cell binding assay. The binding was visualised and quantified

using immunocytochemistry (ICC). Prior to the binding assay, the cytotoxicity of selected compounds was assessed using MTT assay on HEK293 cells. The viabilities of all compounds are excellent with LD<sub>50</sub> > 50  $\mu$ M except compound PBCHM57487213 having LD<sub>50</sub> at around 27  $\mu$ M (ESI Fig. 1†).

In the binding assay, HEK293 cells were incubated with A $\beta$  at a concentration of 1000 pg mL<sup>-1</sup> for 2 hours. The culture medium was then removed and the cells were washed. This was

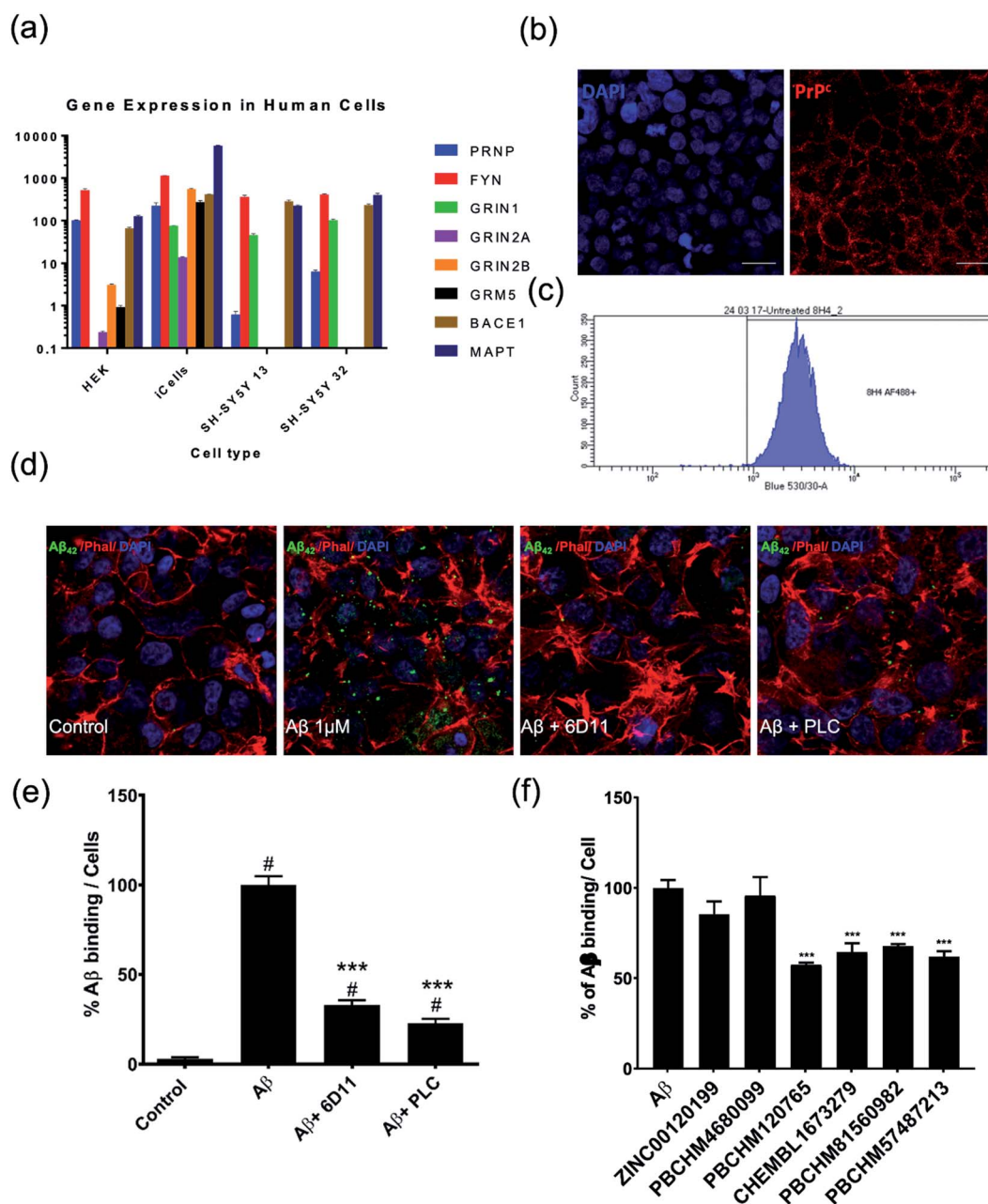


**Fig. 6** Assessment of PrP<sup>C</sup> expression level and A $\beta$  binding to PrP<sup>C</sup> and inhibition of hit compounds. (a) Expression of a selection of neural genes in relevant neural cell lines; (b) HEK293 staining with DAPI (left), PrP<sup>C</sup> antibody 8H4 (right); (c) quantification of PrP<sup>C</sup> in HEK293 by flow cytometry; (d) from left to right: control HEK293 cells, HEK293 cells treated with A $\beta$  at 1000 pg mL<sup>-1</sup> for 2 hours, HEK293 cells treated with A $\beta$  and anti-PrP<sup>C</sup> antibody 6D11, HEK293 cells treated with A $\beta$  and PLC. Cells are stained with anti A $\beta$  antibody (green), Phalloidin (red) and DAPI (blue); (e) quantification of A $\beta$  binding to PrP<sup>C</sup> and inhibition of 6D11 and PLC; (f) percentage of binding of A $\beta$  to PrP<sup>C</sup> on HEK293 in presence and absence of each compounds by immunofluorescence. Values expressed as mean  $\pm$  SD ( $n \geq 3$ ), statistical significance indicated by # $p < 0.05$  in comparison with control groups and \* $p < 0.05$ , \*\* $p < 0.01$ , \*\*\* $p < 0.001$ , \*\*\*\* $p < 0.0001$  in comparison with A $\beta$  treated group, following one-way ANOVA and Tukey's *post-hoc* test.



followed by adding the tested compound in fresh medium at a final concentration of 10  $\mu\text{M}$ . The cells were then left for 1 hour prior to ICC analysis. The percentage of the binding of A $\beta$  in presence and absence of the tested compound is presented in (Fig. 6f). Compounds ZINC00120199 and PBCHM4680099 both showed very little inhibitory effects upon the A $\beta$ -PrP<sup>C</sup> binding while the other 4 compounds all showed clear and statistically

significant inhibition effects. These two compounds seem to have relatively small molecular weight and fewer rotatable bonds.

**The A $\beta$  binders inhibit hyperphosphorylation of Fyn (pFyn) in hiPSC derived neuroprogenitor cell (NPC).** For further functional validation of the hit compounds, appropriate cellular models of biological relevance needed to be developed. HEK293

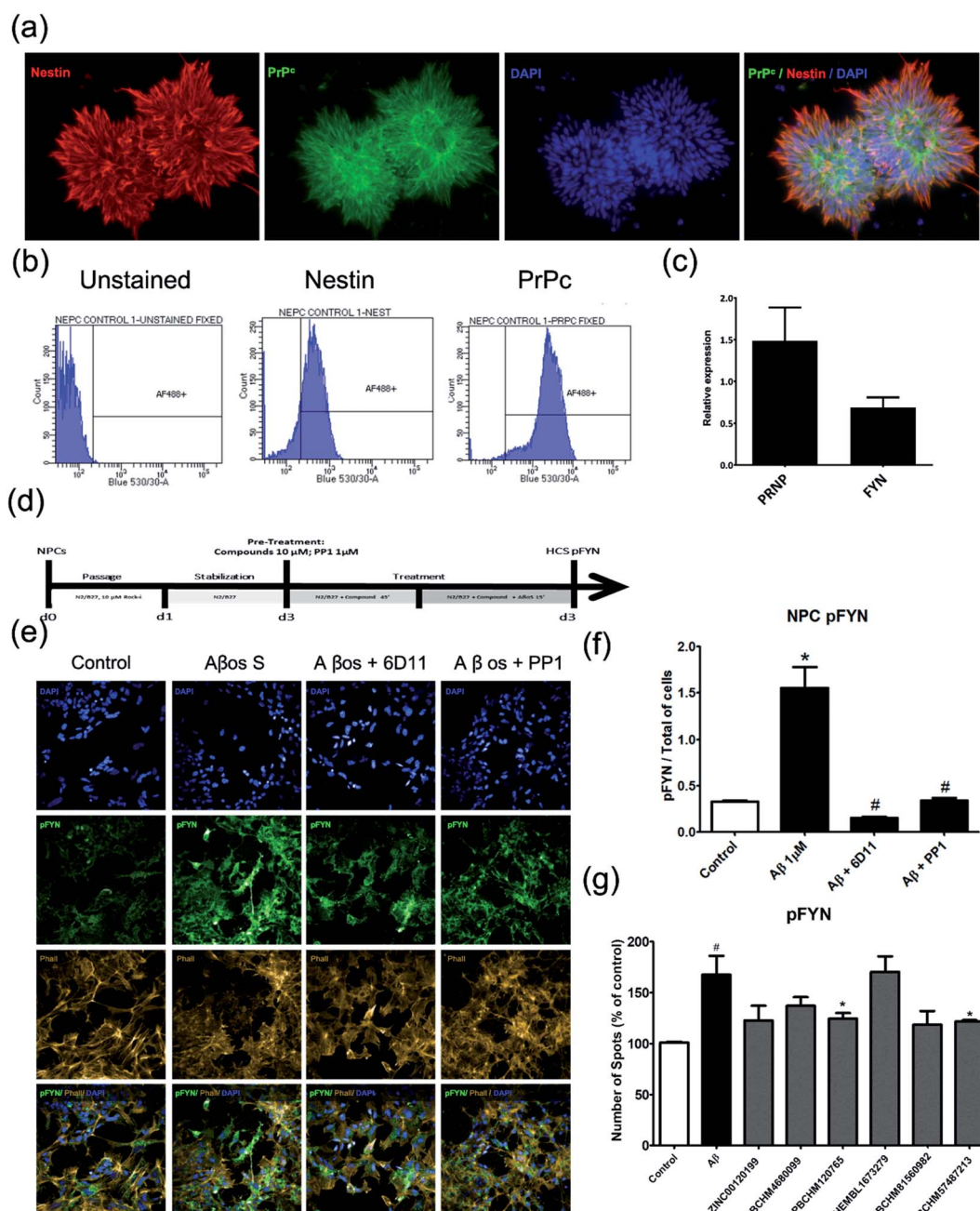


**Fig. 7** pFyn deactivation and kinase activity assay using NPC. (a) Immunofluorescence double staining of NPC for nestin a classical neural progenitor cell marker (red) and anti-prion (green), the nucleus was stained by DAPI (blue) and overlays; (b) confirmation of nestin and PrP<sup>C</sup> expression in NPC cells by flow cytometry. (c) Quantification of PRNP and FYN gene expression in NPC cells by qPCR; (d) compound treatment plan; (e) confirmation of A $\beta$  induced pFYN activation using natural A $\beta$  and inhibition of the pFYN activation by anti-prion antibody (6D11), and PP1 a well-known pFyn inhibitor using immunostaining; (f) quantification of the level of inhibition of pFYN activation with 6D11 and PP1; (g) inhibition of A $\beta$  binders in pFYN activation caused by A $\beta$ ; values expressed as mean  $\pm$  SD ( $n \geq 3$ ), statistical significance indicated by #  $p < 0.05$ , \*  $p < 0.05$ , \*\*  $p < 0.01$ , \*\*\*  $p < 0.001$ , \*\*\*\*  $p < 0.0001$ , following one-way ANOVA and Tukey's *post-hoc* test.



is not appropriate because it is not of neural origin, SH-SY5Y cell lines are human neuronal cell lines, but they don't express all AD signalling pathways. The best choice would then be the iCells neurons however, due to their cost they were not viable for this work. Thus, we developed our own neuronal stem cells models using human iPSC cells. These human neuronal stem cell models are more genetically and functionally relevant to study human neurons than those of animal origins.<sup>65</sup>

To assess the effects of hit compounds on pFyn activity, iPSC-derived NPCs from a health control individual (Cell line MIFF1 [https://web.expasy.org/cellosaurus/CVCL\\_1E69](https://web.expasy.org/cellosaurus/CVCL_1E69)) in under 3 weeks (much shorter than the time it takes to produce natural neurons) and express all essential biomarkers as mature neurons. The expression of the NPC marker, Nestin, and A $\beta$  binding partner, PrP<sup>C</sup>, and PRNP and FYN genes were confirmed using immunostaining (Fig. 7a), flow cytometry (Fig. 7b) and qPCR (Fig. 7c).

The A $\beta$  binders were tested using the same protocol and results are shown (Fig. 7d). The screening protocol was developed using commercial anti-prion antibody, 6D11 and a well-known pFYN inhibitor PP1. 6D11 is a monoclonal anti-mouse IgG against epitope 93–109 on PrP<sup>C</sup> sequence. Recently, this antibody has been found to improve the cognitive deficits in an Alzheimer's disease mice model<sup>63,66,67</sup> and prevent the binding of A $\beta$  to PrP<sup>C</sup> causing Fyn alteration and Tau hyperphosphorylation.<sup>68</sup> We used 6D11 as a positive control for developing the Fyn functional assay. PP1 is a cell-permeable pyrazolopyrimidine compound that is shown to inhibit Src family tyrosine kinases Lck, Fyn, Hck, and Src (IC<sub>50</sub> = 5, 6, 20, and 170 nM, respectively) in *in vitro* kinase assays with an application as an anticancer agent.<sup>69–71</sup>

Both 6D11 and PP1 were used to treat 3 day old NPC in culture for 1 hour prior to A $\beta$  treatment. The cells were harvested for immunofluorescence analysis 15 minutes after the treatment. When compared to the untreated control cells, A $\beta$  caused hyperphosphorylation of Fyn, hence the activation of the Fyn kinase. Both 6D11 and PP1 significantly inhibit the activation of pFyn (Fig. 7e & f). PP1 was chosen as a positive control A $\beta$  binder screening in our pFyn assay as it is a small molecule inhibitor (Fig. 7g). While 5 out of the 6 compounds reduced the Fyn hyperphosphorylation triggered by A $\beta$ , compound **PBCHM9815618** and **PBCHM57487213** produced the most profound effects.

We were specifically interested in pFyn because it is widely expressed in the brain, it is abundant in neurons and it plays an important role in regulating cell proliferation and differentiation during the development of the CNS.<sup>72</sup> It is also involved in signal transduction pathways that regulate survival metabolism and neuronal migration.<sup>73</sup> We focused our studies on the effects of the compounds upon the reduction of the elevated level of pFyn (hyperphosphorylation) because any compound that reduces the pFyn level below the basal levels could be deleterious for the homeostasis of the cells and their mode-of-actions are unrelated to the activation of Fyn caused by the A $\beta$ .

**The A $\beta$  binders reduce the production of phosphorylated Tau (pTau) in mature cortical neurons.** As pTau is the key component in Tau tangles produced in the neurons in the brain

of patients as the result of AD, it is thus a characteristic biomarker. Therefore, in order to test the effects of A $\beta$  binders upon pTau production, mature cortical neurons generated from iPSC from a healthy individual (MIFF1) were obtained after 75 days as previously reported protocol illustrated in Fig. 8a. Key biomarkers for each cell type (DAPI) was used as a general marker for nuclei; SSEA4, Oct4 for iPSC (data not shown); Nestin and PAX6 for NPC (data not shown);  $\beta$ -tubulin III for young neurons and mGlu5 for mature cortical neuron were used to guide the differentiation at each stage prior to full characterizations.

Cells were stained for major protein biomarkers in signalling pathways related to AD development in neurons including general neuronal markers such as  $\beta$ -tubulin 3 ( $\beta$ tub-III) and MAP2, specific glutamatergic markers for cortical neurons such as *N*-methyl D-aspartate receptor subtype 2B (NMDAR2B or NR2B) and mGluR5, PrP<sup>C</sup>, synaptic markers such as synaptophysin (SYP) and PSD-95 (post-synaptic density protein 95) (Fig. 8b). Both NPC and neurons showed positive staining for those markers. The physiological functions of these mature neurons were characterized using electrophysiological functional parameters, *i.e.* action potential (Fig. 8c top) and voltage-gated potassium and sodium ion channel current (Fig. 8c bottom). The data clearly show that iPSCs have been successfully differentiated into mature cortical neurons over an extended period of time and function as normal neurons physiologically. The treatment regime for compounds and A $\beta$  is illustrated in Fig. 8d. Upon the treatment of A $\beta$  binders, significant pTau deposits were clearly seen while the amount of pTau in the untreated control is negligible (Fig. 8e).

Briefly, the iPSC derived nature neurons were passaged and grown for 15 days in B27/BDNF medium, then treated by a mixture of recombinant A $\beta$  at 500 nM and tested compounds at 5 and 10  $\mu$ M. The inhibitory effects of the 6 hit A $\beta$  binders upon the pTau production induced by A $\beta$  can be clearly seen in Fig. 8f. Amongst all A $\beta$  binders, **ZINC0011291995** is the weakest inhibitor, **PBCHM4680099** somewhat displays an inverse dose–response trend. Clearer dose-responses effects can be seen with compounds **PBCHM120765** and **CHEMBL1673279** although **PBCHM120765** seems to be a slightly stronger inhibitor. Inhibitory effects of compounds **PBCHN81560982** and **PBCHM57487213** stayed the same which is similar to that **PBCHM120765** possesses at 10 mM concentration.

Positive outcomes from each assay can be clearly seen from individual cell-based assay. In HEK293 binding assay, 4 out of 6 compounds (**CHEMBL1673279**, **PBCHM57487213**, **PBCHM120765**, and **PBCHM81560982**) showed clear effects in disrupting A $\beta$ –PrP<sup>C</sup> binding through specific binding to A $\beta$  although their direct binding to PrP<sup>C</sup> can not be excluded. Compounds, **PBCHM57487213** and **PBCHM120765** showed noticeable effect in reducing the elevated pFyn level in NPC triggered by A $\beta$  treatment while inhibitory effects of other compounds are observed but not significant. Inhibitory effects on pTau production in mature cortical neurons can be seen with most of the compounds, but statically significant



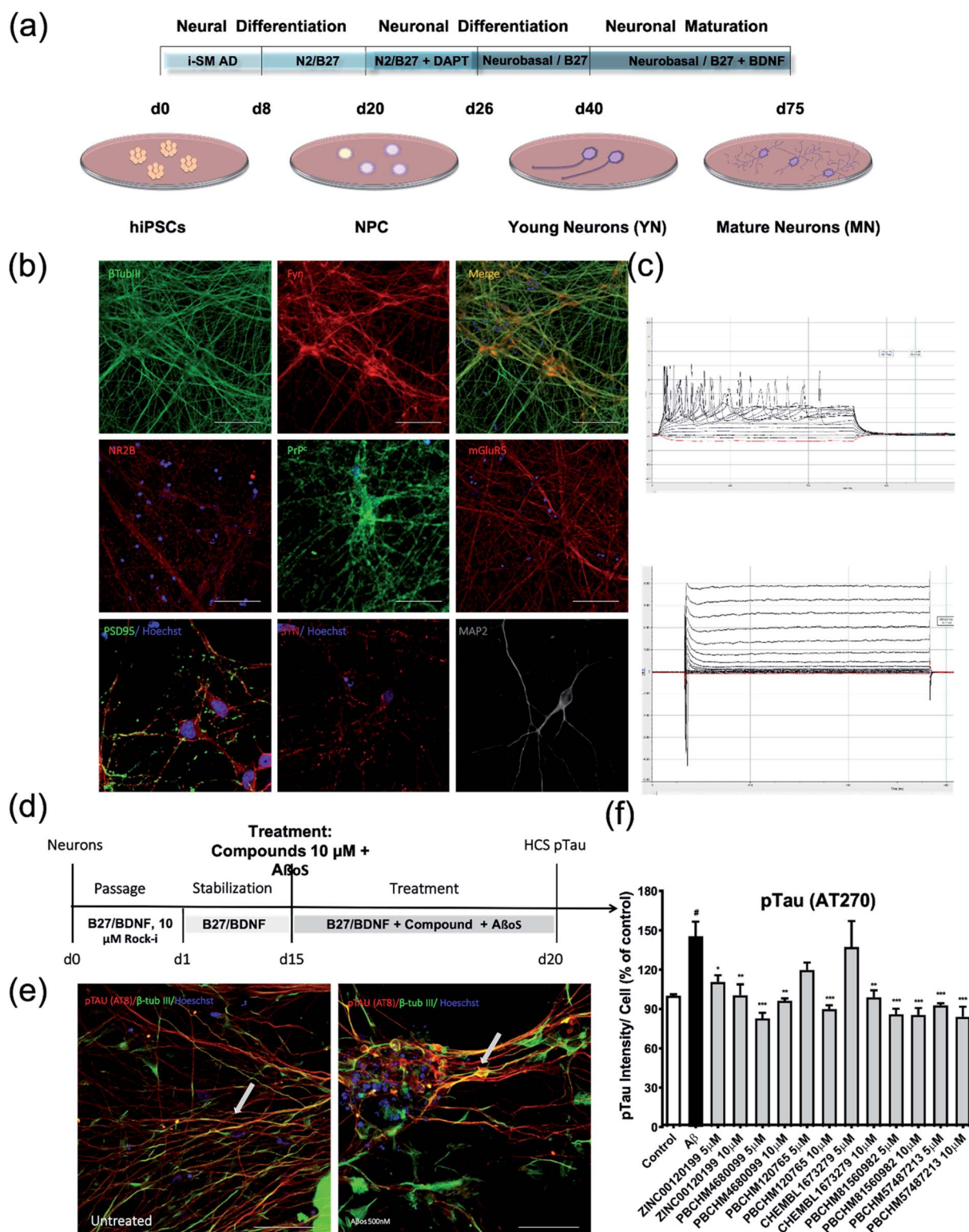


**Fig. 8** pTau assay using mature cortical neurons derived from iPSC. (a) Protocol for differentiating iPSC into neuroprogenitor cells and then mature cortical neurons; (b) characterisation of iPSC derived mature cortical neurons by immunostaining of neuronal markers ( $\beta$ -tubulin III, Fyn, NR2B, PrP<sup>C</sup>, mGluR5, PSD95, SYN and MAP2); (c) electrophysiological characterization of iPSC-derived mature cortical neurons. Action potential (top)  $K^+$ – $Na^+$  ion channel current (bottom) for mature cortical neurons; (d) treatment protocol for A $\beta$  binders for their inhibitory effects on pTau production using mature cortical neurons; (e) pTau production induced by A $\beta$ ; (f) inhibition of pTau by 6 A $\beta$  binders. Values expressed as mean  $\pm$  SD ( $n \geq 3$ ), statistical significance indicated by # $p < 0.05$ , \* $p < 0.05$ , \*\* $p < 0.01$ , \*\*\* $p < 0.001$ , \*\*\*\* $p < 0.0001$ , following one-way ANOVA and Tukey's *post-hoc* test.



Table 4 Ranking of 6 hit compounds cross all three functional assays

Entry	Public ID	Structure	MW	cLog P	PSA	No. of Rotatable bonds	%Inhibition to Abos-PrP <sup>C</sup> binding on HEK293	%Inhibition on pFYN	%Inhibition on pTau	Selected as a hit
1	CHEMBL1673279		343.417	4.5418	20.31	6	34.65	0.59	7.97	N
2	PBCHM4680099		233.242	2.0309	37.38	2	4.20	20.12	43.09	N
3	PBCHM57487213		411.295	3.5695	58.28	7	38.30	27.81	36.30	Y
4	ZINC00120199		243.15	3.1829	26.02	1	14.65	26.04	23.97	N
5	PBCHM120765		203.207	2.5951	26.02	2	42.55	26.63	18.84	N
6	PBCHM81560982		267.59	2.539	66.40	2	32.35	28.40	40.94	Y

inhibitory effects were observed with compounds CHEMBL1673279, PBCHM57487213, PBCHM120765, and PBCHM81560982.

When the data from NMR and biological assays looks a little dispersed which make cross-board comparison a little difficult. In order to give a holistic assessment of the data, activities of all 6 compound under each of the 3 biological experiments were categorised as such 0–10 (red), 10–20 (orange/yellow) and >20 (green). Compounds with cross-board high activities (all >20, in green) were selected as lead compounds (Table 4). The other approach for lead compounds shortlisting was to use results from each one of the 5 assays (<sup>19</sup>F NMR, STD NMR plus 3 biological assays) which was arbitrarily ranked with highest activity assigned 6 and lowest one assigned as 1 in a descend order. The combined rank was produced. The one with the highest value was selected as lead compounds (data not shown). Both approaches yielded the same shortlist of lead compounds two final leads (PBCHM57487213 and PBCHM81560982) were selected after assessment of overall data although compound PBCHM120765 sits on the board line.

Both lead compounds came from the PUBCHEM collection. Both are fluorine-containing small molecules. Compound PBCHM57487213 is a chiral amino alcohol with 2 stereogenic centres. It can be synthesised by the ring opening of appropriately protected epoxide with correct stereo configurations using a trifluoromethyl benzylamine. This compound was patented (US20120053200A1) as a BACE-2 inhibitor which is potential drug target associated with both Alzheimer's diseases and

diabetes. Compound PBCHM81560982 is a simple acylated amino benzoic acid and its biological activity of has not been reported in any literature so far. Both lead compounds are drug-like, obeying Lipinski's and Veber's rules. They can be further optimised and developed into anti-AD drugs. As both compounds have relatively low molecular weight and have some fragment features, an obvious strategy for optimisations could simply be merge these two compounds into one molecule to see if a synergistic activity can be achieved.

These lead structures connect three pillars of Alzheimer's diseases, *i.e.* prion, A $\beta$  and Tau pathways. A $\beta$ o binding is a key feature in A $\beta$  pathway, A $\beta$ o-PrP<sup>C</sup> inhibition connects the A $\beta$  pathway with prion pathway while pTau are key components in Tau pathways and can be triggered by A $\beta$ o and linked with PrP<sup>C</sup> and the activation of Fyn.<sup>68,74</sup> The experiment was designed to test the effects of the hit compounds on the downstream pathways.

## Conclusions

In this work, we sought to identify compounds which bind to soluble A $\beta$ <sub>1-42</sub> oligomers (A $\beta$ o) using a suite of computational, biophysical and biological methods. Soluble A $\beta$ o are the toxic subunits of Alzheimer's disease (AD). A growing body of literature has indicated that the cellular prion protein (PrP<sup>C</sup>) acts as a receptor for A $\beta$ o in AD and connects the A $\beta$  pathway and the Tau pathway. It is expected that A $\beta$ o binders that disrupt the A $\beta$ o and PrP<sup>C</sup> interaction may have effects on downstream



signalling such as Fyn and Tau activities, therefore, possess polypharmacological activities.

Solving the crystal structure of the major disease-causing amyloid peptide, A $\beta$ <sub>1-42</sub> and its oligomers, has proven to be extremely challenging. Most structural information came from solution or solid-state NMR studies. There is neither X-ray crystal structure of A $\beta$ <sub>1-42</sub> in the oligomeric form nor ligand co-crystallised structures being solved so far, although there are several structures of A $\beta$  fibrils (PDB codes: 2MXU, 2LNQ, 6OC9, 6Y1A). This has made structure-based ligand design or high throughput screening unattainable. Therefore, a ligand-based computational approach was developed to rationalize the selection of potential candidate molecules for biophysical and biochemical screening.

With <sup>19</sup>F NMR as a primary screening tool in mind, a computational method was employed that uses fragments of known binders to amyloid proteins to search for compounds containing similar substructures and at least one F-atom in our compiled database of compounds which are in the public domain as well as available in Lilly's internal inventory. 614 soluble compounds out of 971 virtual hits were screened in 91 sub-libraries in <sup>19</sup>F NMR primary screening and 27 compounds were identified as the A $\beta$  binders. Further validation in individual experiments by <sup>19</sup>F NMR against A $\beta$  and against a scrambled A $\beta$ -peptide to eliminate false positives and non-specific binding generated 8 confirmed hits. Further hit expansion on these 8 initial hits produced 36 analogues from which 6 more hits were obtained. This gave a total of 14 hit binders which were taken into the STD NMR experiment.

The STD experiment on the 14 initial hit compounds resulted in 9 confirmed hits. The hot spots which are involved in the binding of the hit compounds to A $\beta$  were mapped out during the STD experiments. Semi-quantitative dose-response curve gave  $K_D$  value at low micromolar levels. The combinations of various experiments using computer-aided design tools, <sup>19</sup>F and STD NMR provided the most stringent assessment of potential binders to A $\beta$ . 6 out of 9 hit binders (**CHEMBL1673279**, **PBCHM4680099**, **PBCHM57487213**, **ZINC00120199**, **PBCHM120765**, and **PBCHM81560982**) were taken forward in the biological evaluation studies.

The compounds were tested in three cellular assays, one measuring A $\beta$ -PrP<sup>C</sup> binding using a HEK293 cell line and the other two assessing changes in the levels of other key AD protein biomarkers including Fyn and Tau using NPC and neurons derived from iPSC. 4 out of 6 compounds (**CHEMBL1673279**, **PBCHM57487213**, **PBCHM120765**, and **PBCHM81560982**) showed good anti-oligomeropathy effects in disrupting A $\beta$ -PrP<sup>C</sup> binding although these compounds did not show direct binding to PrP<sup>C</sup>. The polypharmacological effects of the hit compounds on pFyn and pTau were evaluated in hiPSC derived NPC and cortical neuron models. Compounds **PBCHM57487213** and **PBCHM120765** showed noticeable effect in reducing the elevated pFyn level in NPC triggered by A $\beta$  treatment while inhibitory effects of other compounds were observed but not statistically significantly. Inhibitory effects on pTau production in mature cortical neurons can be seen with most of the compounds, but statistically significant inhibitory

effects were observed with compounds **CHEMBL1673279**, **PBCHM57487213**, **PBCHM120765**, and **PBCHM81560982**.

The two final leads (**PBCHM57487213** and **PBCHM81560982**) were selected after assessment of overall data. The work successfully demonstrated a combined computational, biophysical and biochemical effort in AD drug discovery. The computational method provides a plausible hit rationale for suggesting compounds for NMR screening; <sup>19</sup>F and STD NMR have been shown to be effective tools for validating the compounds suggested by the computational design. Cellular models provided sound biochemical and functional validation of A $\beta$  binders in the anti-oligomeropathy and polypharmacology context. The rate has been improved from 1.3% in initial <sup>19</sup>F NMR screening to 17% in hit expansion, to 62% in STD NMR. A hit rate of 50% was achieved after the biochemical and functional assays. The lead structures that were discovered, connect 3 pillars in Alzheimer's disease pathology, *i.e.* prion, A $\beta$  and Tau pathways. They showed polypharmacological effects on 3 different pathways through specific binding to A $\beta$ , *i.e.* anti-oligomeropathy mechanism. These compounds are drug-like and can be further optimised to produce useful AD therapeutic drugs.

## Conflicts of interest

There are no conflicts to declare.

## Acknowledgements

Studies using human induced pluripotent stem cells were performed in strict accordance with the European Framework 7 Marie Curies guidelines. They are either commercially certified or approved by local institutions. The research leading to these results has received funding from the European Union's Seventh Framework Programme (FP7/2007–2013) under grant agreement no. 612347. The authors are grateful for funding from White Rose University Consortium (WRUC) BBSRC Doctoral Training Programme for Samuel J Dawes; from EPSRC Molecular Scale Engineering DTC for Sasha Stimpson.

## References

- 1 M. Goedert, M. G. Spillantini, B. Ghetti, R. A. Crowther and A. Klug, in *Alzheimer: 100 Years and Beyond*, ed. M. Jucker, K. Beyreuther, C. Haass, R. M. Nitsch and Y. Christen, 2006, pp. 297–304, DOI: 10.1007/978-3-540-37652-1\_38.
- 2 <https://www.alz.co.uk/research/statistics>.
- 3 A. I. Placido, C. M. F. Pereira, A. I. Duarte, E. Candeias, S. C. Correia, R. X. Santos, C. Carvalho, S. Cardoso, C. R. Oliveira and P. I. Moreira, *Biochim. Biophys. Acta, Mol. Basis Dis.*, 2014, **1842**, 1444–1453.
- 4 J. A. Hardy and G. A. Higgins, *Science*, 1992, **256**, 184–185.
- 5 K. Herrup, *Nat. Neurosci.*, 2015, **18**, 794–799.
- 6 D. J. Selkoe and J. Hardy, *EMBO Mol. Med.*, 2016, **8**, 595–608.
- 7 S. Campioni, B. Mannini, M. Zampagni, A. Pensalfini, C. Parrini, E. Evangelisti, A. Relini, M. Stefani,





- C. M. Dobson, C. Cecchi and F. Chiti, *Nat. Chem. Biol.*, 2010, **6**, 140–147.
- 8 B. Mannini, E. Mulvihill, C. Sgromo, R. Cascella, R. Khodarahmi, M. Ramazzotti, C. M. Dobson, C. Cecchi and F. Chiti, *ACS Chem. Biol.*, 2014, **9**, 2309–2317.
- 9 P. Arosio, R. Cukalevski, B. Frohm, T. P. J. Knowles and S. Linse, *J. Am. Chem. Soc.*, 2014, **136**, 219–225.
- 10 G. S. Bloom, *JAMA Neurol.*, 2014, **71**, 505–508.
- 11 H. H. Jarosz-Griffiths, E. Noble, J. V. Rushworth and N. M. Hooper, *J. Biol. Chem.*, 2016, **291**, 3174–3183.
- 12 A. E. Barry, I. Klyubin, J. M. Mc Donald, A. J. Mably, M. A. Farrell, M. Scott, D. M. Walsh and M. J. Rowan, *J. Neurosci.*, 2011, **31**, 7259–7263.
- 13 R. B. DeMattos, K. R. Bales, D. J. Cummins, J. C. Dodart, S. M. Paul and D. M. Holtzman, *Proc. Natl. Acad. Sci. U. S. A.*, 2001, **98**, 8850–8855.
- 14 G. A. N. Crespi, S. J. Hermans, M. W. Parker and L. A. Miles, *Sci. Rep.*, 2015, **5**, 9649.
- 15 A. D. Watt, G. A. N. Crespi, R. A. Down, D. B. Ascher, A. Gunn, K. A. Perez, C. A. McLean, V. L. Villemagne, M. W. Parker, K. J. Barnham and L. A. Miles, *Acta Neuropathol.*, 2014, **127**, 803–810.
- 16 V. L. Villemagne, S. Burnham, P. Bourgeat, B. Brown, K. A. Ellis, O. Salvado, C. Szoëke, S. L. Macaulay, R. Martins, P. Maruff, D. Ames, C. C. Rowe, C. L. Masters and B. Australian Imaging, *Lancet Neurol.*, 2013, **12**, 357–367.
- 17 J. Sevigny, P. Chiao, T. Bussiere, P. H. Weinreb, L. Williams, M. Maier, R. Dunstan, S. Salloway, T. Chen, Y. Ling, J. O'Gorman, F. Qian, M. Arastu, M. Li, S. Chollate, M. S. Brennan, O. Quintero-Monzon, R. H. Scannevin, H. M. Arnold, T. Engber, K. Rhodes, J. Ferrero, Y. Hang, A. Mikulskis, J. Grimm, C. Hock, R. M. Nitsch and A. Sandrock, *Nature*, 2016, **537**, 50–56.
- 18 J. Toyn, *Expert Rev. Clin. Pharmacol.*, 2015, **8**, 267–269.
- 19 M. S. Parihar and T. Hemnani, *J. Clin. Neurosci.*, 2004, **11**, 456–467.
- 20 B. De Strooper, R. Vassar and T. Golde, *Nat. Rev. Neurol.*, 2010, **6**, 99–107.
- 21 R. J. O'Brien and P. C. Wong, in *Annual Review of Neuroscience, Vol 34*, ed. S. E. Hyman, T. M. Jessell, C. J. Shatz, C. F. Stevens and H. Y. Zoghbi, 2011, vol. 34, pp. 185–204.
- 22 S. T. Ferreira, M. V. Lourenco, M. M. Oliveira and F. G. De Felice, *Front. Cell. Neurosci.*, 2015, **9**, 191.
- 23 T. Bilousova, C. A. Miller, W. W. Poon, H. V. Vinters, M. Corrada, C. Kawas, E. Y. Hayden, D. B. Tepow, C. Glabe, R. Albay III, G. M. Cole, E. Teng and K. H. Gylys, *Am. J. Pathol.*, 2016, **186**, 185–198.
- 24 T. Yang, S. Li, H. Xu, D. M. Walsh and D. J. Selkoe, *J. Neurosci.*, 2017, **37**, 152–163.
- 25 M. Costanzo and C. Zurzolo, *Biochem. J.*, 2013, **452**, 1–17.
- 26 M. Jucker and L. C. Walker, *Nat. Neurosci.*, 2018, **21**, 1341–1349.
- 27 S.-J. Lee, P. Desplats, C. Sigurdson, I. Tsigelny and E. Masliah, *Nat. Rev. Neurol.*, 2010, **6**, 702–706.
- 28 B. B. Holmes and M. I. Diamond, *J. Biol. Chem.*, 2014, **289**, 19855–19861.
- 29 J. Lauren, D. A. Gimbel, H. B. Nygaard, J. W. Gilbert and S. M. Strittmatter, *Nature*, 2009, **457**, 1128–U1184.
- 30 K. O'Neill, S. H. Chen and R. D. Brinton, *Exp. Neurol.*, 2004, **188**, 268–278.
- 31 J. Luis Herrera, C. Fernandez, M. Diaz, D. Cury and R. Marin, *Steroids*, 2011, **76**, 840–844.
- 32 S. V. Salazar, C. Gallardo, A. C. Kaufman, C. S. Herber, L. T. Haas, S. Robinson, J. C. Manson, M. K. Lee and S. M. Strittmatter, *J. Neurosci.*, 2017, **37**, 9207–9221.
- 33 C. Li and J. Gotz, *EMBO J.*, 2017, **36**, 3120–3138.
- 34 P. Joshi, S. Chia, J. Habchi, T. P. J. Knowles, C. M. Dobson and M. Vendruscolo, *ACS Comb. Sci.*, 2016, **18**, 144–153.
- 35 C. Dalvit, *Prog. Nucl. Magn. Reson. Spectrosc.*, 2007, **51**, 243–I.
- 36 J. H. Byun, H. Kim, Y. Kim, I. Mook-Jung, D. J. Kim, W. K. Lee and K. H. Yoo, *Bioorg. Med. Chem. Lett.*, 2008, **18**, 5591–5593.
- 37 K. N. Dahlgren, A. M. Manelli, W. B. Stine, L. K. Baker, G. A. Krafft and M. J. LaDu, *J. Biol. Chem.*, 2002, **277**, 32046–32053.
- 38 I. Kuperstein, K. Broersen, I. Benilova, J. Rozenski, W. Jonckheere, M. Debulpaep, A. Vandersteen, I. Segers-Nolten, K. Van der Werf, V. Subramaniam, D. Braeken, G. Callewaert, C. Bartic, R. D'Hooge, I. C. Martins, F. Rousseau, J. Schymkowitz and B. De Strooper, *EMBO J.*, 2010, **29**, 3408–3420.
- 39 T. J. Esparza, N. C. Wildburger, H. Jiang, M. Gangolli, N. J. Cairns, R. J. Bateman and D. L. Brody, *Sci. Rep.*, 2016, **6**, 38187.
- 40 E. Y. Hayden and D. B. Teplow, *Alzheimers Res. Ther.*, 2013, **5**, 60.
- 41 G.-f. Chen, T.-h. Xu, Y. Yan, Y.-r. Zhou, Y. Jiang, K. Melcher and H. E. Xu, *Acta Pharmacol. Sin.*, 2017, **38**, 1205–1235.
- 42 R. Gniadecki, C. Assaf, M. Bagot, R. Dummer, M. Duvic, R. Knobler, A. Ranki, P. Schwandt and S. Whittaker, *Br. J. Dermatol.*, 2007, **157**, 433–440.
- 43 K. H. Dragnev, W. J. Petty, S. J. Shah, L. D. Lewis, C. C. Black, V. Memoli, W. C. Nugent, T. Hermann, A. Negro-Vilar, J. R. Rigas and E. Dmitrovsky, *Clin. Cancer Res.*, 2007, **13**, 1794–1800.
- 44 F. J. Esteva, J. Glaspy, S. Baidas, L. Laufman, L. Hutchins, M. Dickler, D. Tripathy, R. Cohen, A. DeMichele, R. C. Yocum, C. K. Osborne, D. F. Hayes, G. N. Hortobagyi, E. Winer and G. D. Demetri, *J. Clin. Oncol.*, 2003, **21**, 999–1006.
- 45 C. Di Scala, H. Chahinian, N. Yahi, N. Garmy and J. Fantini, *Biochemistry*, 2014, **53**, 4489–4502.
- 46 Z. Mirza and M. A. Beg, *Curr. Alzheimer Res.*, 2017, **14**, 327–334.
- 47 H. Pham Dinh Quoc, T. Nguyen Quoc, Z. Bednarikova, P. Le Huu, L. Huynh Quang, Z. Gazova and M. S. Li, *ACS Chem. Neurosci.*, 2017, **8**, 1960–1969.
- 48 N. Bibi, S. M. Danish Rizvi, A. Batool and M. A. Kamal, *Curr. Pharmaceut. Des.*, 2019, **25**(27), 2989–2995.
- 49 B. G. Jenkins, *Life Sci.*, 1991, **48**, 1227–1240.
- 50 J. Oravcova, V. Mlynarik, S. Bystricky, L. Soltes, P. Szalay, L. Bohacik and T. Trnovec, *Chirality*, 1991, **3**, 412–417.
- 51 H. Chen, S. Viel, F. Ziarelli and L. Peng, *Chem. Soc. Rev.*, 2013, **42**, 7971–7982.



- 52 C. Dalvit, P. E. Fagerness, D. T. A. Hadden, R. W. Sarver and B. J. Stockman, *J. Am. Chem. Soc.*, 2003, **125**, 7696–7703.
- 53 C. Dalvit and A. Vulpetti, *Magn. Reson. Chem.*, 2012, **50**, 834.
- 54 T. Zhu, S. Y. Cao, P. C. Su, R. Patel, D. Shah, H. B. Chokshi, R. Szukala, M. E. Johnson and K. E. Hevener, *J. Med. Chem.*, 2013, **56**, 6560–6572.
- 55 C. Dalvit, A. D. Gossert, J. Coutant and M. Piotta, *Magn. Reson. Chem.*, 2011, **49**, 199–202.
- 56 M. Mayer and B. Meyer, *Angewandte Chemie-International Edition*, 1999, **38**, 1784–1788.
- 57 M. Mayer and B. Meyer, *J. Am. Chem. Soc.*, 2001, **123**, 6108–6117.
- 58 A. Farrugia, *Transfus. Med. Rev.*, 2010, **24**, 53–63.
- 59 P. J. Loll, B. S. Selinsky, K. Gupta and C. T. Sharkey, *Worldwide Protein Data Bank*, 2001, DOI: 10.2210/pdb1eqg/pdb.
- 60 B. S. Selinsky, K. Gupta, C. T. Sharkey and P. J. Loll, *Biochemistry*, 2001, **40**, 5172–5180.
- 61 C. Peters, M. P. Espinoza, S. Gallegos, C. Opazo and L. G. Aguayo, *Neurobiol. Aging*, 2015, **36**, 1369–1377.
- 62 J. W. Um, H. B. Nygaard, J. K. Heiss, M. A. Kostylev, M. Stagi, A. Vortmeyer, T. Wisniewski, E. C. Gunther and S. M. Strittmatter, *Nat. Neurosci.*, 2012, **15**, 1227–U1285.
- 63 E. Chung, Y. Ji, Y. J. Sun, R. J. Kascsak, R. B. Kascsak, P. D. Mehta, S. M. Strittmatter and T. Wisniewski, *BMC Neurosci.*, 2010, **11**, 130.
- 64 A. Muller, C. Kloppel, M. Smith-Valentine, J. Van Houten and M. Simon, *Biochim. Biophys. Acta Biomembr.*, 2012, **1818**, 117–124.
- 65 R. Dolmetsch and D. H. Geschwind, *Cell*, 2011, **145**, 831–834.
- 66 J. E. Pankiewicz, S. Sanchez, K. Kirshenbaum, R. B. Kascsak, R. J. Kascsak and M. J. Sadowski, *Mol. Neurobiol.*, 2019, **56**, 2073–2091.
- 67 J. F. McEwan, M. L. Windsor and S. D. Cullis-Hill, *Tumor Biol.*, 2009, **30**, 141–147.
- 68 M. Larson, M. A. Sherman, F. Amar, M. Nuvolone, J. A. Schneider, D. A. Bennett, A. Aguzzi and S. E. Lesne, *J. Neurosci.*, 2012, **32**, 16857.
- 69 A. H. Sikkema, S. H. Diks, W. F. A. den Dunnen, A. ter Elst, F. J. G. Scherpen, E. W. Hoving, R. Ruijtenbeek, P. J. Boender, R. de Wijn, W. A. Kamps, M. P. Peppelenbosch and E. de Bont, *Cancer Res.*, 2009, **69**, 5987–5995.
- 70 R. Karni, S. Mizrahi, E. Reiss-Sklan, A. Gazit, O. Livnah and A. Levitzki, *FEBS Lett.*, 2003, **537**, 47–52.
- 71 J. H. Hanke, J. P. Gardner, R. L. Dow, P. S. Changelian, W. H. Brissette, E. J. Weringer, K. Pollok and P. A. Connelly, *J. Biol. Chem.*, 1996, **271**, 695–701.
- 72 S. Schenone, C. Brullo, F. Musumeci, M. Biava, F. Falchi and M. Botta, *Curr. Med. Chem.*, 2011, **18**, 2921–2942.
- 73 S. J. Parsons and J. T. Parsons, *Oncogene*, 2004, **23**, 7906–7909.
- 74 L. A. Gomes, S. A. Hipp, A. R. Upadhaya, K. Balakrishnan, S. Ospitalieri, M. J. Koper, P. Largo-Barrientos, V. Uytterhoeven, J. Reichwald, S. Rabe, R. Vandenberghe, C. A. F. von Arnim, T. Tousseyn, R. Feederle, C. Giudici, M. Willem, M. Staufienbiel and D. R. Thal, *Acta Neuropathol.*, 2019, **138**, 913–941.

